CANADIAN CLIMATE CENTRE

REPORT NO. 89-8

# The Application of AES Environmental Data to Ice Interaction Modelling

*Final Report*

ATMOSPHERIC ENVIRONMENT SERVICE

DOWNSVIEW, ONTARIO

1989

THIS REPORT HAS RECEIVED ONLY LIMITED CIRCULATION BECAUSE OF THE SPECIAL NATURE OF THE PROJECT. HOWEVER, REFERENCE IS PERMITTED IF THE WORDS "UNPUBLISHED MANUSCRIPT" ARE MADE PART OF THE BIBLIOGRAPHIC ENTRY, IN ACCORDANCE WITH ACCEPTED PRACTICE.

**OTHER CANADIAN CLIMATE CENTRE (CCC)**
**SCIENTIFIC SERIES INCLUDE:**

1. CS series - CCC Climatological Study
2. CLI series - CCC Climatological Memoranda
3. CDS/DS series - CCC Climatic Data Summary
   - CCC Documentation Sheet

For further information on climatological publications contact the

Climatological Services Division
Atmospheric Environment Service
4905 Dufferin Street
Downsview, Ontario M3H 5T4

# THE APPLICATION OF AES ENVIRONMENTAL DATA TO ICE INTERACTION MODELLING

FINAL REPORT

Submitted to

CANADIAN CLIMATE CENTRE
ATMOSPHERIC ENVIRONMENT SERVICE
ENVIRONMENT CANADA

by

Ian Jordaan and Associates Inc.
St. John's
Newfoundland

December 1988

Project Team

Richard McKenna
Alfred Marshall
Ian Jordaan

This work was supported by the Federal Panel on Energy Research and Development (PERD)

A publication of the Canadian Climate Program

## ABSTRACT

The role of the AES data bases for calculating extreme ice loads on offshore structures is addressed and particular attention is focussed on the Sea Ice Climate Information System (CRISP). Landfast and pack ice sites in the Beaufort Sea are used to illustrate the appropriate extremal probabilistic techniques. Initially, critical ice load scenarios are defined and seasons for which each scenario applies are determined from the data. Probability distributions of the geometrical features of the pack ice and of the ice velocity are calculated. Where processes are combined, design parameters are obtained by combining probability distributions, e.g. by convolution of the constituent environmental parameter distributions. Emphasis is also placed on extremal probabilistic methods. Since maximum ice loads are specific to structure design, representative parameters such as floe kinetic energy and momentum are calculated. The method used to obtain distributions of extreme loading conditions is based on stochastic independence of events and requires the estimation of arrival rates of critical events. Extension to the case of exchangeability can be achieved by considering parameter uncertainty. Other features of the study include the updating of velocity distributions conditional upon collision with the structure.

Because of the ease of access to digital data bases of ice concentration, CRISP is particularly useful for establishing seasons that correspond to ice loading scenarios. Ice cover information can also be used in conjunction with meteorological data for estimating pack ice and landfast ice movements. At present, ice motion and floe geometry data are not available in the data bases for the drilling areas in the nearshore Beaufort Sea; their inclusion would assist in obtaining design loads for ice.

# RÉSUMÉ

On étudie le rôle des bases de données du SEA dans le calcul des charges extrêmes de glace dans les constructions au large des côtes, en insistant sur le Système d'information mer-glace-climat (CRISP). On se sert des emplacements de glace de rive et de banquise de la mer de Beaufort pour illustrer les techniques probabilistes des extrêmes. Au début, on définit les scénarios critiques de charges de glace et on détermine, d'après les données, les saisons d'application de chacun des scénarios. On calcule la distribution probabiliste des caractéristiques géométriques de la banquise et de la vitesse des glaces. Quand on combine les processus, on obtient les paramètres types en combinant les distributions de probabilités, par convolution des distributions des paramètres constitutifs d'environnement. On insiste aussi sur les méthodes probabilistes des extrêmes. Vu que les charges maximales de glace se rattachent à la conception des constructions, on calcule des paramètres représentatifs, comme l'énergie et le moment cinétiques des floes. La méthode utilisée pour obtenir les distributions des conditions extrêmes de charges repose sur l'indépendance stochastique des phénomènes et nécessite l'estimation des dates d'apparition des phénomènes critiques. Pour étendre la méthode au cas d'échangeabilité, on peut étudier l'incertitude des paramètres. Les autres éléments de l'étude comprennent la mise à jour des distributions de vitesses, sous réserve d'une collision avec la construction.

Du fait de la facilité d'accès des bases de données numériques sur la concentration des glaces, CRISP est particulièrement utile pour établir les saisons qui correspondent aux scénarios de charges de glace. Pour estimer les mouvements de la glace de banquise et de rive, on peut aussi utiliser, conjointement avec les données météorologiques, des renseignements sur la couverture de glace. A l'heure actuelle, les bases ne donnent pas de données sur le mouvement des glaces et la géométrie des floes pour les zones de forage de la mer de Beaufort situées près de la côte. Leur inclusion aiderait à obtenir les charges types de glace.

## ACKNOWLEDGEMENTS

This study was conducted as a result of a contract administered by Canadian Climate Centre, Atmospheric Environment Service, Environment Canada. The writers wish to express their gratitude to Tom Agnew, who acted as scientific authority, for his assistance and advice during the conduct of the study.

# TABLE OF CONTENTS


| | Page |
|---|---|
| ABSTRACT | i |
| ACKNOWLEDGEMENTS | iii |
| TABLE OF CONTENTS | iv |
| 1. INTRODUCTION AND SCOPE | 1 |
| 1.1 Design for Ice Environments | 1 |
| 1.2 Definition of Ice Load Scenarios | 5 |
| 1.3 AES Data Bases: Amauligak and Kaubvik Sites | 10 |
| 2. PROBABILISTIC MODELLING | 17 |
| 2.1 General Aspects of Modelling | 17 |
| 2.2 Extremal Statistics: Frequency of Occurrence | 20 |
| 2.3 Incorporation of Data | 24 |
| 2.4 Estimation of Arrival Rates and Expected Number of Arrivals | 25 |
| 2.5 Bayesian Updating Conditional on Collision | 29 |
| 3. MODELLING OF ENVIRONMENT | 32 |
| 3.1 Overview | 32 |
| 3.2 Ice Load Modelling | 34 |
| 3.3 Season Lengths | 37 |
| 3.4 First Year Ice Thickness | 40 |
| 3.5 Wind Induced Ice Drift | 44 |
| 4. DURATION OF SCENARIOS FROM AES DATA | 55 |
| 4.1 Data Sources | 55 |
| 4.2 Ice Concentration Criteria for Season Boundaries | 55 |
| 4.3 Ice Thickness Freeze-up Criterion | 58 |
| 4.4 Landfast Ice Season | 63 |
| 4.5 Season Lengths | 65 |
| 5. LANDFAST ICE INTERACTION | 69 |
| 5.1 Landfast Ice Processes and Loads | 69 |
| 5.2 Landfast Ice Thickness | 70 |
| 5.3 Landfast Ice Events | 71 |
| 5.4 Landfast Ice Speed | 79 |
| 5.5 Future Characterization of Landfast Ice Processes | 82 |

TABLE OF CONTENTS (Cont'd)


| | | Page |
|---|---|---|
| 6. | FIRST YEAR PACK ICE INTERACTION | 85 |
| | 6.1 Ice Concentration | 85 |
| | 6.2 Ice Speed Distributions | 87 |
| | 6.3 Thickness of Moving First Year Ice | 93 |
| | 6.4 First Year IceLoad Example | 94 |
| 7. | MULTIYEAR ICE | 99 |
| | 7.1 Multiyear Ice Events | 99 |
| | 7.2 Multiyear Ice Concentration | 100 |
| | 7.3 Multiyear Ice Speeds | 103 |
| | 7.4 Multiyear Floe Characteristics | 104 |
| | 7.5 Multiyear Ice Load Example | 107 |
| 8. | CONCLUSIONS AND RECOMMENDATIONS | 112 |
| | 8.1 Concluding Remarks | 112 |
| | 8.2 Recommendations | 115 |
| 9. | REFERENCES | 119 |

# 1. INTRODUCTION AND SCOPE

## 1.1 Design for Ice Environments

There is a variety of ice conditions in the arctic that must be considered in the design of offshore structures. Figure 1.1 shows some of these conditions in winter; the ice can be landfast or moving in the polar pack, with the shear and transition zones between the two. Multiyear floes can be present in summer or winter and constitute a considerable hazard. More rarely, ice islands, or fragments thereof, move through the Beaufort Sea. Design will focus on extreme ice events and some severe interactions that have been observed.

The most dramatic case of an extreme ice event is the interaction of a multiyear ice floe with the Molikpaq structure at the Amauligak I-65B site on April 12, 1986. The structure was evacuated during the event. Considerable vibrations occurred and the sand core began to flow from the interior of the caisson.

Load combinations also represent an important area of concern. A recorded case of combined wind and ice action is the incident concerning the steel Caisson Retained Island (CRI) at the Kadluk O-07 location during January 1984. High wind drove ice up against the caisson walls and some overtopping of the wave deflectors resulted, likely due to combination of landfast ice breaking off, and unusually strong south west wind. Another incident occurred while the single steel drilling caisson (SSDC) was at

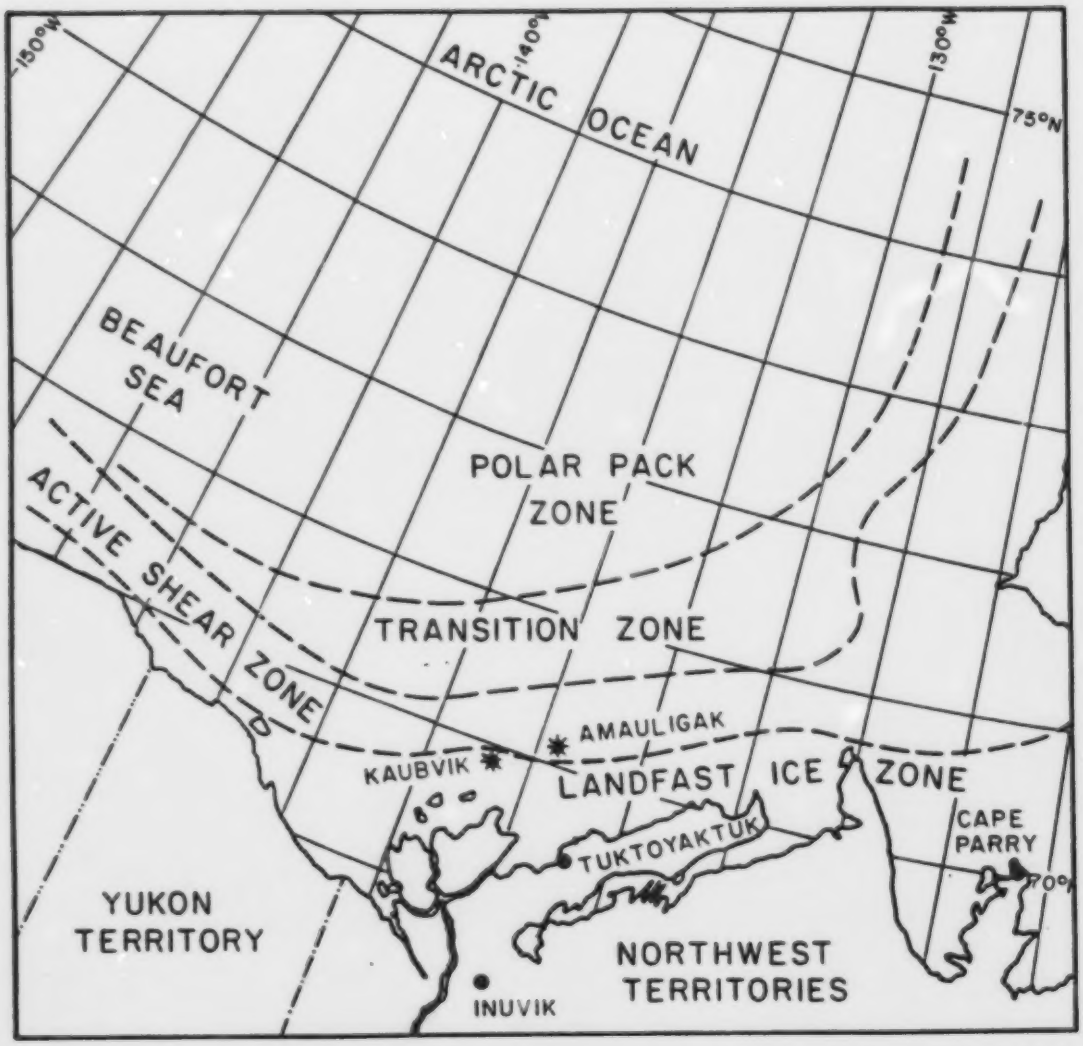


Figure 1.1 Variety of ice conditions in the winter in the Canadian Beaufort Sea

Kogyuk N-67. The rig was partially evacuated as a result of a massive ice floe driven by high winds. The floe was grounded on ice rubble and minor damage was done to a cantilever support beam.

The object of engineering design for offshore structures is to ensure that the design resistance exceeds the applied load by a reasonable margin. In traditional design this was achieved by a "factor of safety", equal to resistance divided by load. The values would typically be in the range from 1.5 to 2.0. This approach does not explicitly recognise the uncertainties in the design process. These relate to the fact that it is not in general possible to specify unique values of either load or resistance.

The direction of development of engineering practice has been to recognise the situation formally (and appropriately) by the use of probability theory. Figure 1.2 shows schematically a distribution for load and resistance. The load would correspond to the maximum load in a period of time, for instance a year. The safety embodied in the design procedure can then be related formally to the probability of failure $p_f$ or the reliability $(1-p_f)$ per annum.

The determination of the probability distribution for environmental ice loads is the focus of the present report. It represents an essential step in determining design criteria, i.e. in specifying design loads that are adequate from the point of view of safety.

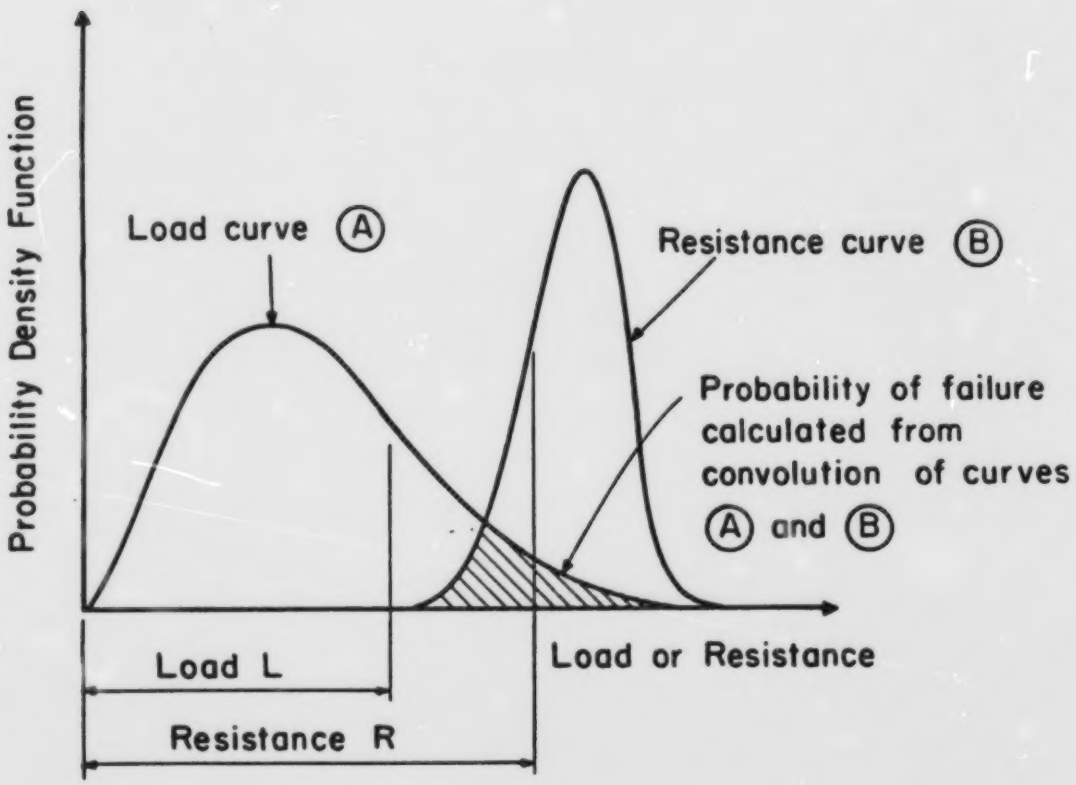


Figure 1.2 The basic design problem. The present project is concerned with determining the probability density for environmental loads.

## 1.2 Definition of Ice Load Scenarios

It is important to capture the essential features of ice-structure interactions in a set of cases, for which the parameter inputs and the calculation of each load or pressure are identical. The overall framework that has been adopted (in draft form) for the CSA standard is illustrated in Figure 1.3. The role of the ice loading scenarios is clearly illustrated. For the present work, the framework has been defined to be that shown in Figure 1.4, since the mechanics of the ice-structure interaction have not been considered. The main emphasis in the present work is the link between the environment (wind, temperature, ice concentration, .... ) and the ice events of interest.

After consultation with AES, the scenarios illustrated in Table 1.1 were decided upon for the present study. Apart from ice island collisions, they represent the principal scenarios of interest in considering ice-structure interaction in the Beaufort Sea.

The landfast ice scenario (FL) only occurs adjacent to shore during the winter season. This scenario is characterized by fixed slowly moving ice, generally reaching maximum speeds of only a few meters per day. The critical design events are when motion results from storm winds or when a significant portion of landfast ice breaks off and moves with the neighbouring pack ice. The appropriate design parameters and the AES environmental data that are relevant to this load scenario are given in Table 1.2. Air temperature can influence both thermal strains in the ice

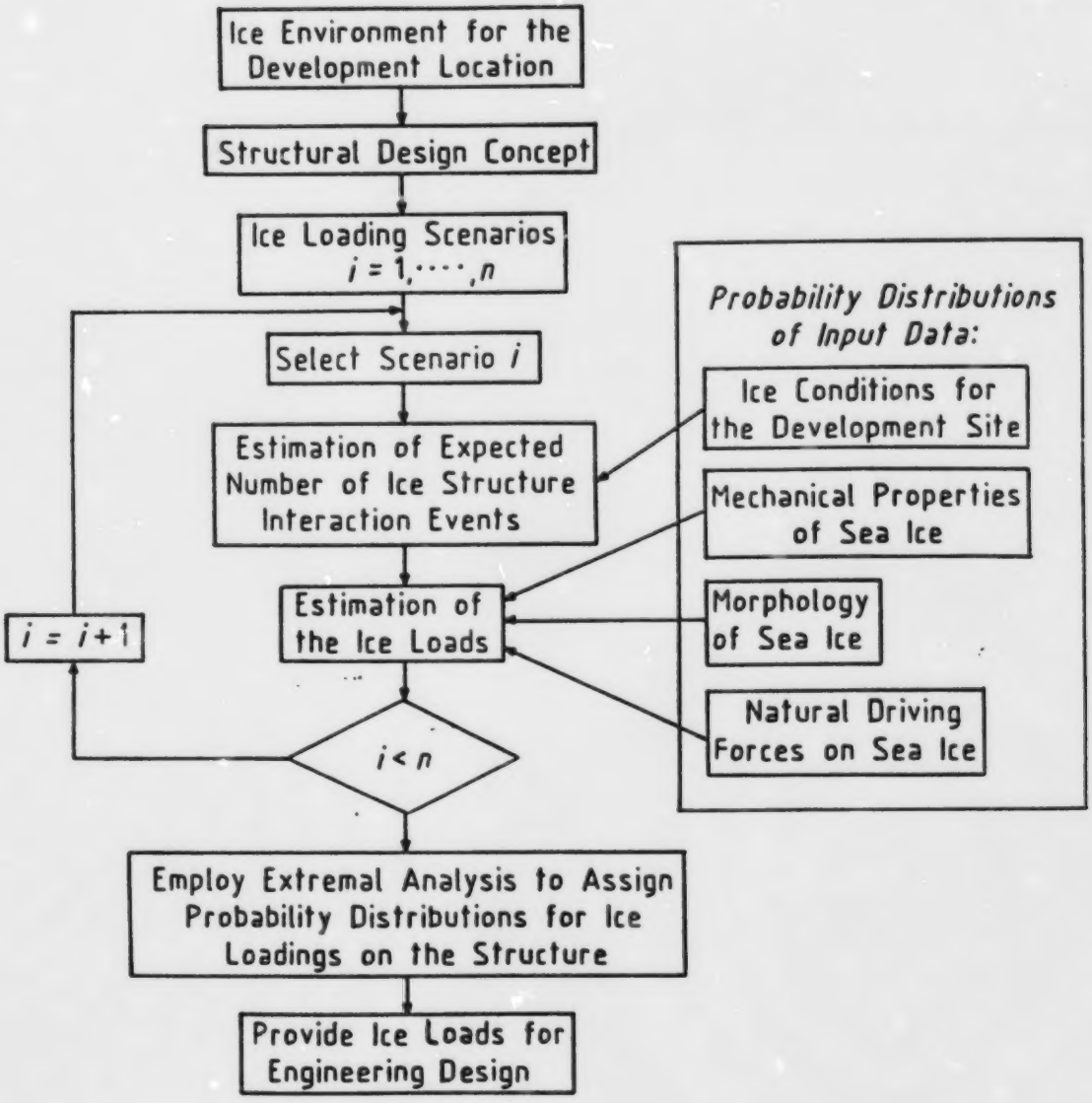
Ice Environment for the Development Location
Structural Design Concept
Ice Loading Scenarios
i = 1,···,n
Select Scenario i
Estimation of Expected Number of Ice Structure Interaction Events
Estimation of the Ice Loads
i = i+1
i < n
Employ Extremal Analysis to Assign Probability Distributions for Ice Loadings on the Structure
Provide Ice Loads for Engineering Design
Probability Distributions of Input Data:
Ice Conditions for the Development Site
Mechanical Properties of Sea Ice
Morphology of Sea Ice
Natural Driving Forces on Sea Ice

Figure 1.3 A general framework for the probabilistic approach (CSA draft Standard S.471)

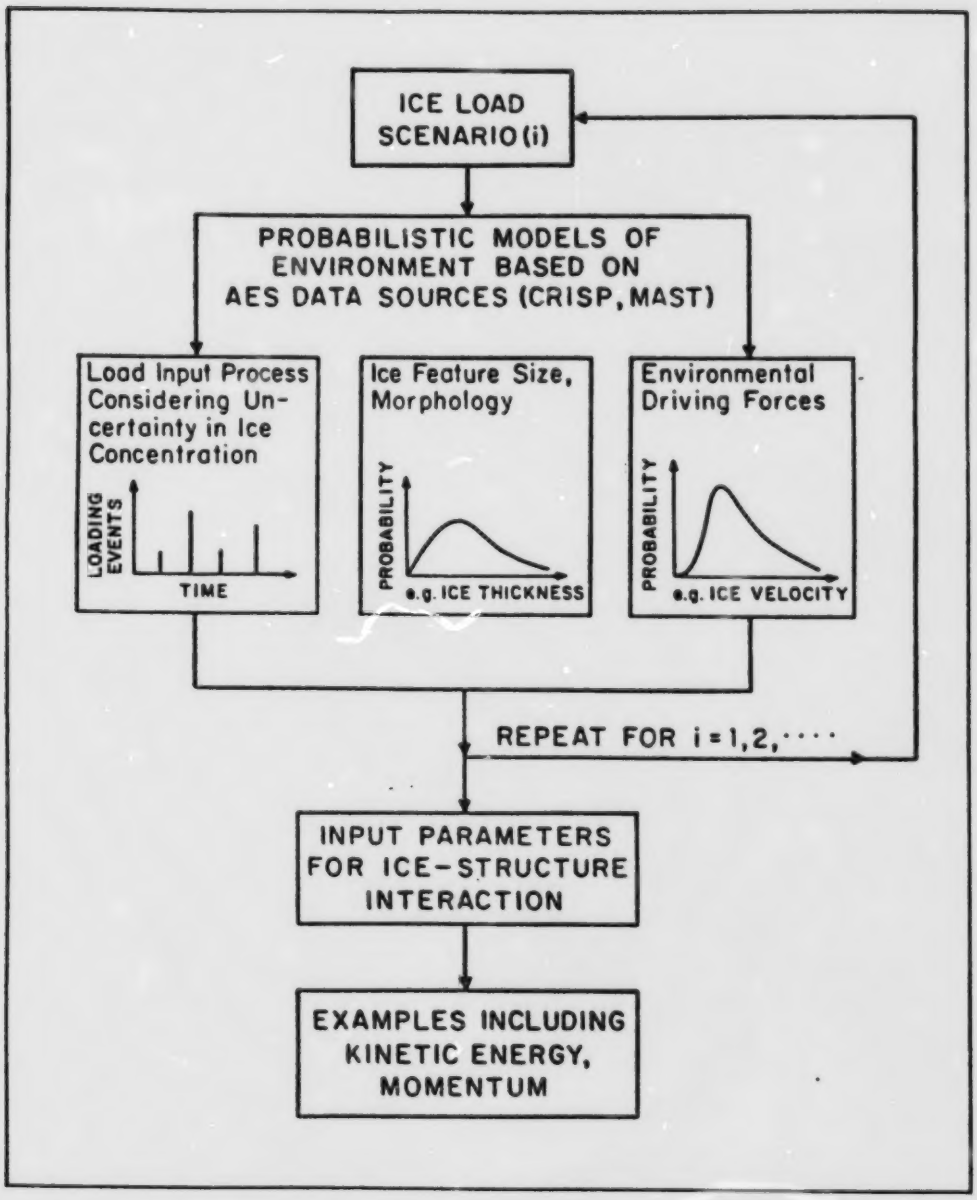
ICE LOAD SCENARIO (i)
PROBABILISTIC MODELS OF ENVIRONMENT BASED ON AES DATA SOURCES (CRISP, MAST)
Load Input Process Considering Uncertainty in Ice Concentration
LOADING EVENTS
TIME
Ice Feature Size, Morphology
PROBABILITY
e.g. ICE THICKNESS
Environmental Driving Forces
PROBABILITY
e.g. ICE VELOCITY
REPEAT FOR i = 1,2,····
INPUT PARAMETERS FOR ICE-STRUCTURE INTERACTION
EXAMPLES INCLUDING KINETIC ENERGY, MOMENTUM

Figure 1.4 Logic of the approach for the present study

Table 1.1 Ice Loading Scenarios

| Season | Ice Type | Scenario |
|---|---|---|
| Winter | First year (FY) | FL Landfast Ice (water depth < 25-30 m) |
| | First year (FY) | FP Pack Ice (water depth > 15-20 m) |
| | Multiyear (MY) | MP Multiyear floes in first year pack ice |
| Summer | Multiyear (MY) | MS Freely floating multiyear floes |

Table 1.2 Landfast Ice Load Scenario (FL)

| Event | Design Parameters | Relevant AES Environmental Data |
|---|---|---|
| Storm | Ice thickness<br>Ice displacement<br>Ice velocity<br>Frequency of movements<br>Ice properties for creep and damage | Ice thickness<br>Air temperature<br>Wind: speed and duration |
| Break-off | Ice thickness<br>Frequency of events<br>Duration of events<br>Ice preparation for creep and damage | Ice thickness<br>Air temperature<br>Wind: speed, direction |

and the thickness of the landfast ice. Storm and break off events are essentially wind driven.

Freely floating first year ice (FP) can impact offshore structures at any point during the course of the year. This scenario is most critical later in the winter when the ice has achieved a thickness of greater than 1 m and may be the result of wind driven motion or due to ice pack forces pushing floes lodged against the structure. When consolidated, first year ridges can also be a hazard. The parameters relating to this scenario are described in Table 1.3.

The multiyear scenarios MP and MS described in Tables 1.4 and 1.5 differ from the first year situations in that the key design parameter is the multiyear ice concentration. This parameter is used to compute the arrival rate for multiyear floes. The summer scenario is simplified since, once a floe is lodged against the structure, there is no adjacent pack ice to exert forces that can cause creep events.

## 1.3 AES Data Bases: Amauligak and Kaubvik Sites

The ice load scenarios described in Section 1.2 are based on conditions in the Canadian Beaufort Sea. One of the unique features of this area is the transition from landfast ice to the active shear zone and the multiyear pack ice. Much of the exploration activity takes place in the area inshore and just offshore of the 20 m depth contour that is the outer extent of the landfast ice in winter. Two sites were selected to illustrate

Table 1.3 First Year Winter Ice Load Scenario (FP)

| Event | Design Parameters | Relevant AES Environmental Data |
|---|---|---|
| FY moving ice | FY ice thickness<br>Ice velocity<br>Ice crushing parameters<br>Ice flexure parameters | Air temperature<br>Ice thickness<br>Ice concentration<br>Wind: speed, direction, duration |
| FY stationary ice (creep) | FY ice thickness<br>Ice creep parameters<br>Creep-crushing transition | Air temperature |
| FY ridges | Ice velocity<br>Ridge density<br>Ridge geometry<br>Rubble strength<br>Creep-crushing transition | Ice concentration<br>Wind |

Table 1.4 Winter Load Scenario for Multiyear Floes in First Year Ice (MP)

| Event | Design Parameters | Relevant AES Environmental Data |
|---|---|---|
| MY moving ice | MY ice thickness<br>Ice velocity<br>MY floe size<br>MY ice concentration<br>MY ice crushing properties<br>MY ice flexure properties<br>Added mass<br>FY ice crushing properties<br>FY ice flexure properties | FY ice concentration<br>FY ice thickness<br>Wind: speed, direction, duration<br>MY ice concentration |
| MY ice creep | MY ice thickness<br>Ice velocity<br>MY ice concentration<br>MY ice creep properties<br>FY ice creep properties | MY ice concentration<br>FY ice concentration<br>Wind: speed, direction, duration |
| MY ridges | Ridge frequency<br>Ridge geometry<br>MY ice concentration<br>Ice velocity<br>MY ice crushing properties | MY ice concentration<br>FY ice concentration<br>Wind: speed, direction, duration |

Table 1.5 Summer Load Scenario for Freely Floating Multiyear Ice Floes (MS)

| Event | Design Parameters | Relevant AES Environmental Data |
|---|---|---|
| MY moving ice | MY ice thickness<br>Ice velocity<br>MY floe size<br>MY ice concentration<br>MY ice crushing properties<br>MY ice flexure properties | Wind<br>MY ice concentration |
| MY ridges | MY ridge frequency<br>MY ridge geometry<br>MY ice concentration<br>Ice velocity | Wind<br>MY ice concentration |

the extremal analysis procedure for determining ice loads. Situated in 14 m of water, Kaubvik (69.9°N, 135.4°W) becomes landfast during most winters. In contrast, Amauligak (70.1°N, 133.9°W) lies in the active shear zone, seldom landfast and subject to the encroachment of multiyear pack ice in winter. These sites are approximately 80 km apart and are situated offshore in the Beaufort Sea 80 km and 125 km respectively from Tuktoyaktuk as illustrated in Figure 1.1.

The calculation of ice design loads at sites such as these is assisted using AES (Atmospheric Environment Service) digital data bases that can be accessed by CRISP (Climate Research for Ice Software Package) and MAST (Marine Statistics Software Package) and DUST (Duration Statistics Package). The data bases contain fundamental ice and meteorological information in standard formats.

CRISP deals with ice cover data, snow cover data and temperature data necessary for ice growth calculations. This analysis tool emphasises both the spatial and temporal information and makes available a wide range of statistical measures, including means, variances and cumulative values of probability distributions. Many different graphical formats for their presentation are provided. The two primary sources of data accessed by CRISP are the NOAA-Navy Joint Ice Center charts coded according to the World Meteorological Standard SIGRID (Sea Ice Grid) and the AES Regional data bases covering the east coast, Hudson Bay and the Canadian arctic (Agnew et al, 1987; Sea Ice Climate Information System, 1986).

The SIGRID data set was digitized from weekly NOAA - Navy Joint Ice Centre ice charts for 1972 to 1984. It provides all year coverage of first year and multiyear ice concentrations at grid points separated by distances of no greater than 28 km (15 nautical miles). The SIGRID data are used in this study for determining season boundaries based on ice coverage and for determining wind induced ice motion.

The AES Regional ice data span the years 1960 to 1980 and provide first year and multiyear ice concentrations digitized from the weekly AES ice charts. The resolution varies since the information has been sythesized to a staggered grid but the largest separation between data points is 45 km. Since the data only cover the summer months between June and October on a regular basis, the SIGRID source is preferred for establishing season boundaries. Ice concentrations differ between the two sources for the multiyear ice and for the first year ice during season transitions. These differences are discussed in later sections of this report.

The MAST package accesses marine weather data from coastal stations, floating buoys and drill ships. For the Beaufort Sea, drill ships and artificial islands provide the only accurate meteorological information at offshore sites. Hourly meteorological data were obtained for the Amauligak site for June to October 1981, September 1983 to July 1984 and September to November 1985. At Tuktoyaktuk, an hourly time series was available during the period between 1972 and 1985, except during the initial years when hourly information was only recorded during daylight hours. Air temperature

data were required for ice growth calculations and winds were used for estimating ice motion.

# 2. PROBABILISTIC MODELLING

## 2.1 General Aspects of Modelling

One of the refreshing consequences of the probabilistic analysis of loads on arctic structures has been the increased emphasis on modelling, as against data analysis and reduction. No doubt, this has resulted from a shortage of records, and the absence of techniques that are analogous to hindcasting. The result has been that the construction of models, and the reasons and assumptions underlying them, have been given more thought.

As an example of the preceding, consider the standard extremal (double exponential) distribution. The most general formulation of the theory, as regards parameter estimation, is based on exchangeability (de Finetti, 1974; Jordaan and Maes, 1984). To pursue this further, we consider a series of events of interest during a season, such as storms. We will denote these events as $(E_1, E_2, \ldots, E_i, \ldots)$. Associated with the events are random quantities, for instance peak ice speeds, or floe diameters or ice loads. For any particular quantity of interest, and it could be any of the set of environmental quantities that occur at points in time, we denote the series of values as $(X_1, X_2, X_3, \ldots, X_i, \ldots)$. Each $X_i$ can be thought of as an individual value, e.g. floe diameter, or as a peak value e.g. the maximum ice speed during storm "i" during the occurrence of an event, $E_i$.

The basic condition of exchangeability is that we do not consider the order of the results $(X_1, X_2, \ldots)$ to be of importance in making our

probabilistic judgements. This seems to be very reasonable; another way of looking at this is to permute the set of results $(X_i)$ and to make the judgement that the permuted set, $(X^{(i)})$ say, is of equal validity as a data set.

The engineering problem is that of studying the maximum[1] of the series of values $X_1, X_2, \ldots$ . Denoting this value as Z, we are interested in

$$Z = \max(X_1, X_2, \ldots, X_i, \ldots) \tag{2.1}$$

The values of X are random (uncertain) and they have a probability density function (pdf) denoted $f_X(x)$. The distribution of X is called the parent distribution. Since X is random, so is Z. The problem of obtaining the distribution of Z from that of X is essentially one of extremal statistics. The pdf and distribution function of Z are denoted $f_Z(z)$ and $F_Z(z)$ respectively. This process is illustrated in Figure 2.1.

Often the number of quantities $X_i$ in equation (2.1) is large and the probability distribution of Z tends to the double exponential distribution (see equation (2.3) in the next section). This limiting distribution is valid under quite wide conditions, similar to those for the central limit theorem (which is based on sums, rather than extremes, of quantities such as those in equation (2.1)). The statement is sometimes made that there is no reason to chose one distribution over another for modelling extremes. On

---

[1]Sometimes, we are interested instead in the minimum. This problem is a variant of the one discussed above, and treated in a similar way.

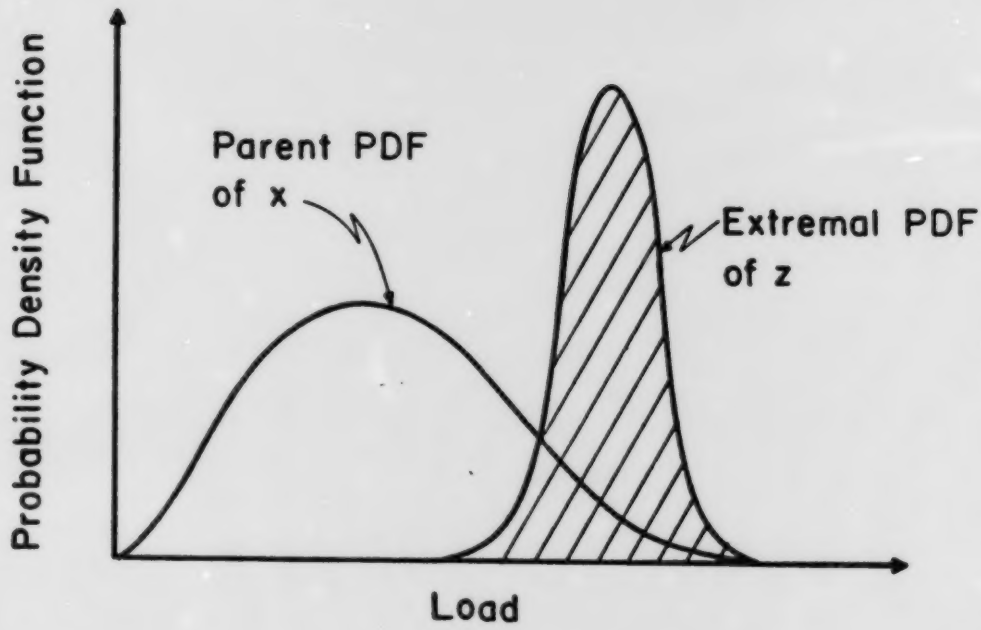


Figure 2.1 Extremal probability density function

the contrary, the natural process being modelled is often analogous to the assumptions underlying the derivation of equation (2.3) - more so if exchangeability is used rather than the usual assumption of independent and identically distributed random quantities.

In the same way, often the Poisson distribution will be a natural way to model the number of events $E_i$ in a given interval of time. The assumptions underlying this distribution are wider than is sometimes assumed; for instance the rate of arrival need not be constant and can even vary as a step during the interval under consideration (Snyder, 1975). The Poisson distribution is related to the Peak Over Threshold (POT) method which is very useful in ice load estimation.

## 2.2 Extremal Statistics: Frequency of Occurrence

In classical extremal analysis, as noted above, the number of quantities $X_i$, say n, in equation (2.1) is large. This is not generally so, and it is important to appreciate this fact. The expected number of quantities in equation (2.1) can be large or small, even less than one (ice islands have a "return period" of more than a thousand years).

Therefore the following classification is made:

(1) Rare events.

(2) Frequent events, usually associated with continuous processes such as wave action.

(3) Occasional events.

1. Rare events. These are defined so that the probability of occurrence is small enough for the probability of more than one event per year to be neglected, i.e. there will be at most one value in the set $(X_1, X_2, \ldots)$ of equation (2.1). The extremal distribution is derived by simple scaling as shown in Figure 2.2 in which $\nu$ = expected number of events in the year ($\nu \ll 1$). The extremal distributions are characterised by a spike of mass $(1-\nu)$ at the origin, and a diffuse tail to the right.

2. Frequent events. By contrast, the extremal distribution is narrow and peaked. If the number of peak quantities $X_i$ in equation (2.1) is n, i.e. i=1, 2, ..., n, then the distribution of the extreme Z has the distribution function

$$F_Z(z) = F_x^n(z) \qquad (2.2)$$

where $F_X(x)$ is the distribution function for x. Equation (2.2) is based on the usual assumption that the $X_i$'s can be modelled as independent and identically distributed (i.i.d.) random quantities and that all $X_i$'s are less than z, noting that $Pr(X_i \leq z) = F_X(z)$. The process of shifting the parent distribution to a more peaked extreme is illustrated in Figure 2.1.

If n is very large, the distribution of Z tends to the asymptotic extremal distribution,

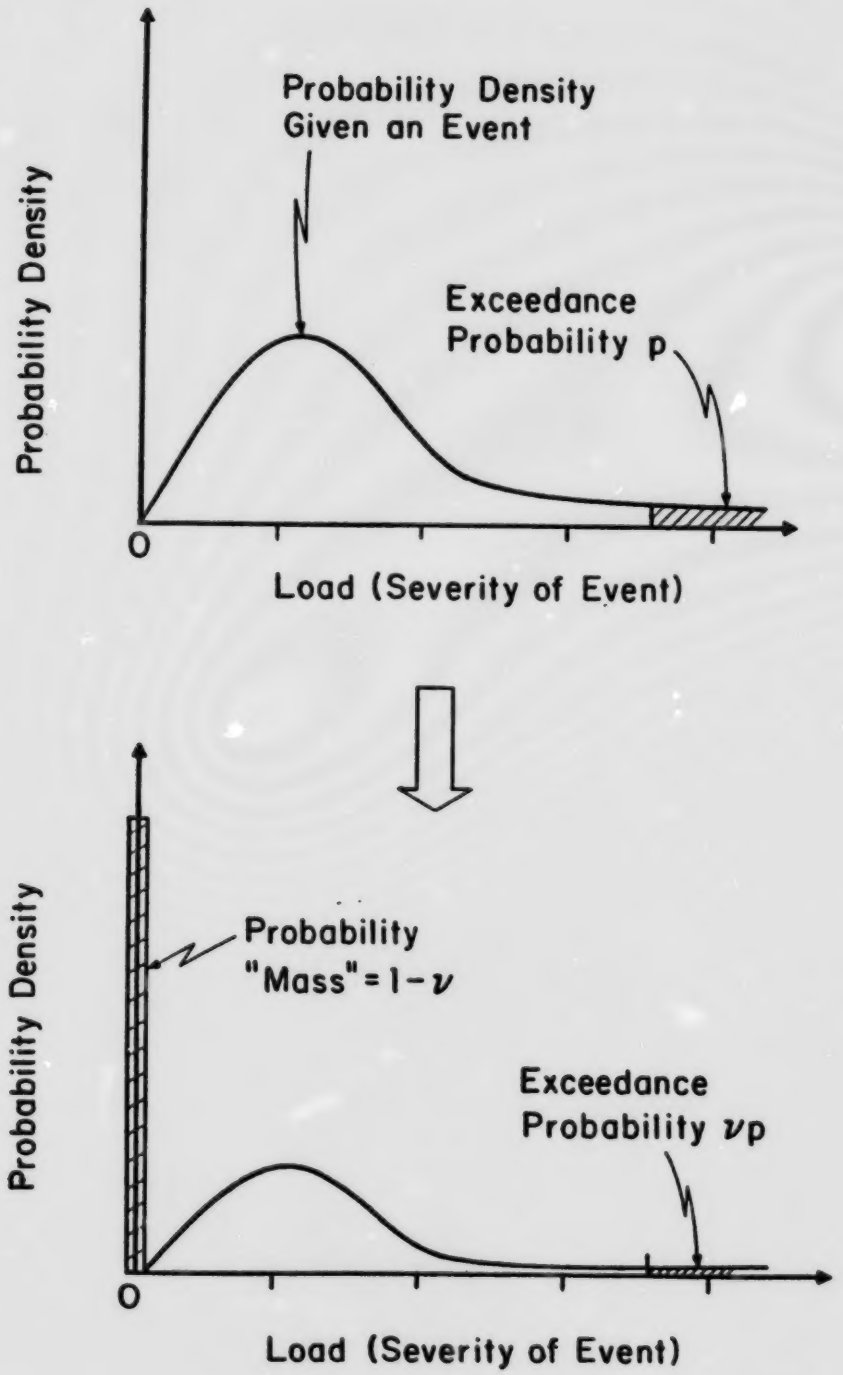


Figure 2.2 Extreme distribution for rare events

$$\text{i.e. } F_Z(z) = \exp\left[-e^{-\alpha(z-u)}\right] \tag{2.3}$$

where $\alpha$ and u are parameters of the distribution. It is important to emphasize that this is intended as a distribution for the quantity of interest. The point of emphasis here is that there are good mathematical-physical reasons to postulate that the extreme value of the quantity of interest can be modelled by the distribution function of the form of equation (2.3). (The determination of the parameters is not addressed in this comment; an analogy would be the use of the central limit theorem and the Gaussian distribution in modelling natural averaging processes, with subsequent parameter determination).

3. Occasional events. In this case n is not large. It may be random: then it is written as N. The extremal distribution is given by

$$F_Z(z) = \sum_{\text{all } n} F_X^n(z) p_n \tag{2.4}$$

where $p_n$ is Pr(N=n). If N is Poisson-distributed, often a convenient assumption, then

$$\Pr(N=n) = p_n = \frac{e^{-\nu}\nu^n}{n!}, \quad n=0,1,2,\ldots \tag{2.5}$$

where $\nu$ = expected number of events. The cumulative distribution function of Z may be obtained as

$$F_Z(z) = \exp[-\nu(1-F_X(z))], \qquad (2.6)$$

where $\nu$ is again the expected number of events in the year (or time period of interest). Equation (2.6) may be derived on the following basis. Consider events amongst the $E_i$ for which $X>z$. The expected number of arrivals for these will be a proportion of the number $\nu$ for all events, i.e.

$$\nu \rightarrow \nu[1 - F_X(z)].$$

Now equation (2.6) is just the value of the Poisson distribution, equation (2.5), with the rate $[\nu(1-F_X(z)]$ and with n=0. This is the probability of no quantities $X_i$ being greater than z, i.e. all $X_i \leq z$, as required.

The model just described is highly relevant to the analysis of ice load events. The use of the Poisson process and equation (2.6) has a direct relation to the Peak-over-Threshold (POT) method (Baird et al, 1986).

## 2.3 Incorporation of Data

The previous section dealt with the question of basic probabilistic modelling. Usually, the inclusion of data is aimed at the estimation of parameter values (Baird et al, 1986, for example). The concept of exchangeability as introduced in section 2.1 results in a model which amounts to the usual i.i.d. model but with parameters of the model themselves treated as randon quantities. For example the distribution given by equation (2.3) would still apply (under similar assumptions of large n,

etc.) but the parameters $\alpha$, u would be random. Figure 2.3 shows schematically the probability distribution for a parameter of distribution, denoted A. The distribution of A would be updated by any available information I. Thus

$$f_{A|I}(a) = \frac{L(I|A=a)}{N} * f_A(a) \qquad (2.7)$$

where $L$ is a likelihood function,

N is a normalising constant,

and $f_A(a)$ is the probability density function.

All interpretations of parameter estimation can be seen as parts of a more complete theory (de Finetti, 1974). Starting with a diffuse prior distribution, i.e. $f_A(a) \propto$ constant, then the moments are one way of finding point estimates, e.g. $\mu_A$ could be the mean. The method of maximum likelihood consists of using the mode of the distribution $f_{A|I}$. The best method is to treat A as random and to integrate over its parameter space.

Another important aspect of data, if the model of equation (2.6) is to be used, is the estimation of the expected number of arrivals, $\nu$. This will be dealt with in the following section.

## 2.4 Estimation of Arrival Rates and Expected Number of Arrivals

The arrivals of ice floes, ridges, or in general, ice features can be modelled as a Poisson process; as noted this gives a simple and elegant

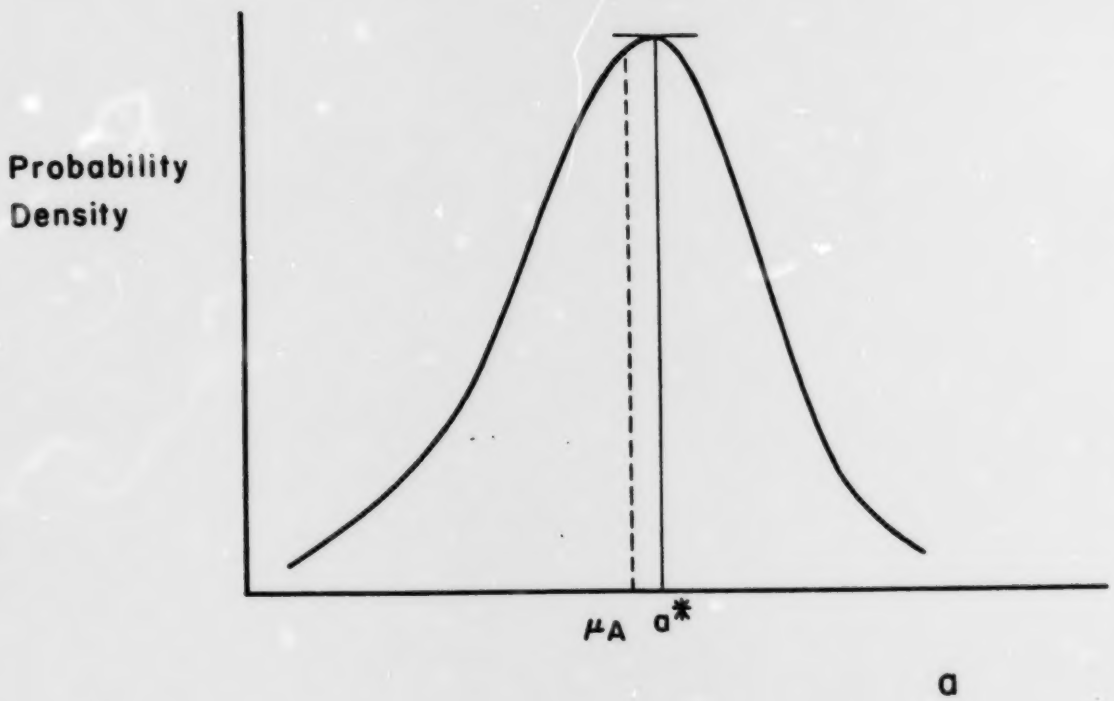


Figure 2.3 Uncertainty regarding a parameter A of a distribution; $a^*$ is the maximum likelihood estimator of A.

formulation for the extremal distribution function (equation (2.6)). The expected number of arrivals, $\nu$ or alternatively, the mean arrival rate, $\bar{\lambda}$, is given by:

$$\nu = \int_0^t \lambda(\tau)\, d(\tau) = \bar{\lambda} t \tag{2.8}$$

where $\lambda(\tau)$ is the arrival rate (intensity), at time $\tau$, and t = total time under consideration.

For ice features that cover an area such as floes, as against lineal features such as ridges, the following analysis is appropriate. The following notation is used (see Figure 2.4)

- B is the lateral dimension of ice feature, at right angles to velocity. B is random with probability density function (pdf), $f_B(b)$;
- A is the area of ice feature, with pdf $f_A(a)$;
- V is the velocity of the ice feature, with pdf $f_v(v)$;
- C is the concentration (proportion of surface covered by ice category under consideration), with pdf $f_C(c)$;

  Velocity and concentration can be correlated, with joint pdf $f_{C,V}(c,v)$;
- R is the density of ice features, i.e. the number per unit area, with pdf $f_R(r)$; and
- w is the width of the structure.

For a short period of time $\Delta t$,

$$\Pr(\text{collision}) = \lambda(t)\Delta t = r(b + w)\, v\Delta t \tag{2.9}$$

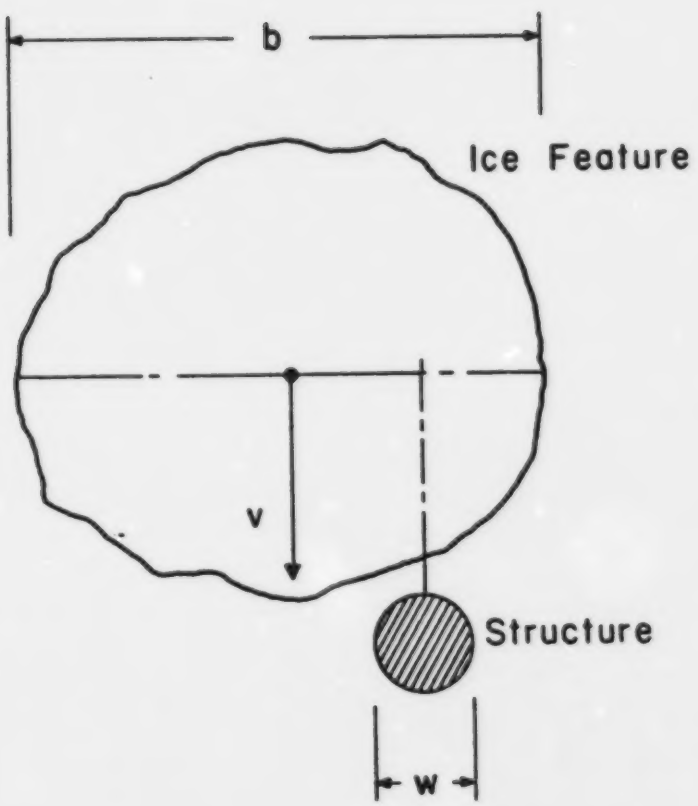


Figure 2.4 Ice feature showing the projected width normal to its direction of motion

If the probability distributions, $f_{C,V}(c,v)$ and $f_B(b)$ reflect the changing conditions during the total interval of time considered (e.g. concentration changes with time), then

$$\bar{\lambda} = \iiint \frac{c}{a} (b + w)\, v\, f_{C,V}(c,v)\, f_B(b)\, dc\, db\, dv \qquad (2.10)$$

in which stochastic independence is assumed of B with respect to C and V (this assumption could be avoided if necessary) and furthermore

$$\bar{\lambda} = \frac{\bar{b} + w}{a} \iint cv\, f_{C,V}(c,v)\, dcdv$$

$$\bar{\lambda} = \frac{\bar{b} + w}{a} (\bar{c}\,\bar{v} + \sigma_{CV}),$$

where the bars denote mean values and $\sigma_{CV}$ = covariance between C and V. Note that $\sigma_{CV} = \sigma_C \sigma_V \rho_{CV}$, where $\rho_{CV}$ is the correlation coefficient.

## 2.5 Bayesian Updating Conditional on Collision

The necessity to update certain random quantities such as speed, size of ice feature, conditional on a collision with a structure is important for fixed structures (Jordaan, 1983; see also Dunwoody, 1983). Taking the speed V as an example, and letting the symbol C denote the extent of a collision, Bayes' theorem is applied as follows:

$$p_{v|c}(v|c) = \frac{p(C|v)\ p_v(v)}{N} \qquad (2.11)$$

where $p_v$ is the generic distribution and N is a normalising constant. Since $p(C|v) \propto v$, the distribution $p_{v|c}$ is different from $p_v$.

The use of the gamma distribution results in an interesting further simplification. The Bayesian updating of equation (2.11) and the use of $p(C|v) \propto v$, as discussed above, results in a new gamma distribution with the shape parameter $\alpha$ changed to $\alpha+1$. Typical results are shown in Figure 2.5.

The two-parameter gamma distribution is given by

$$f_v(v) = \frac{v^{\alpha-1} e^{-v/\beta}}{\beta^{\alpha}\,\Gamma(\alpha)}\ ,\ v \geq 0 \qquad (2.12)$$

where the velocity V is the random quantity being modelled, $\alpha$ = shape parameter and $\beta$ = scale parameter. Note that $\alpha$ and $\beta > 0$. Applying equation (2.11) with $p(C|v) \propto v$, we have

$$f_{v|c}(v) = \frac{1}{N}\, v^{\alpha} e^{-v/\beta} \qquad (2.13)$$

where N is a normalising constant; equation (2.13) is also of the gamma family, with shape parameter equal to $\alpha+1$. The factor $N = 1/[\beta^{\alpha+1}\Gamma(\alpha+1)]$.

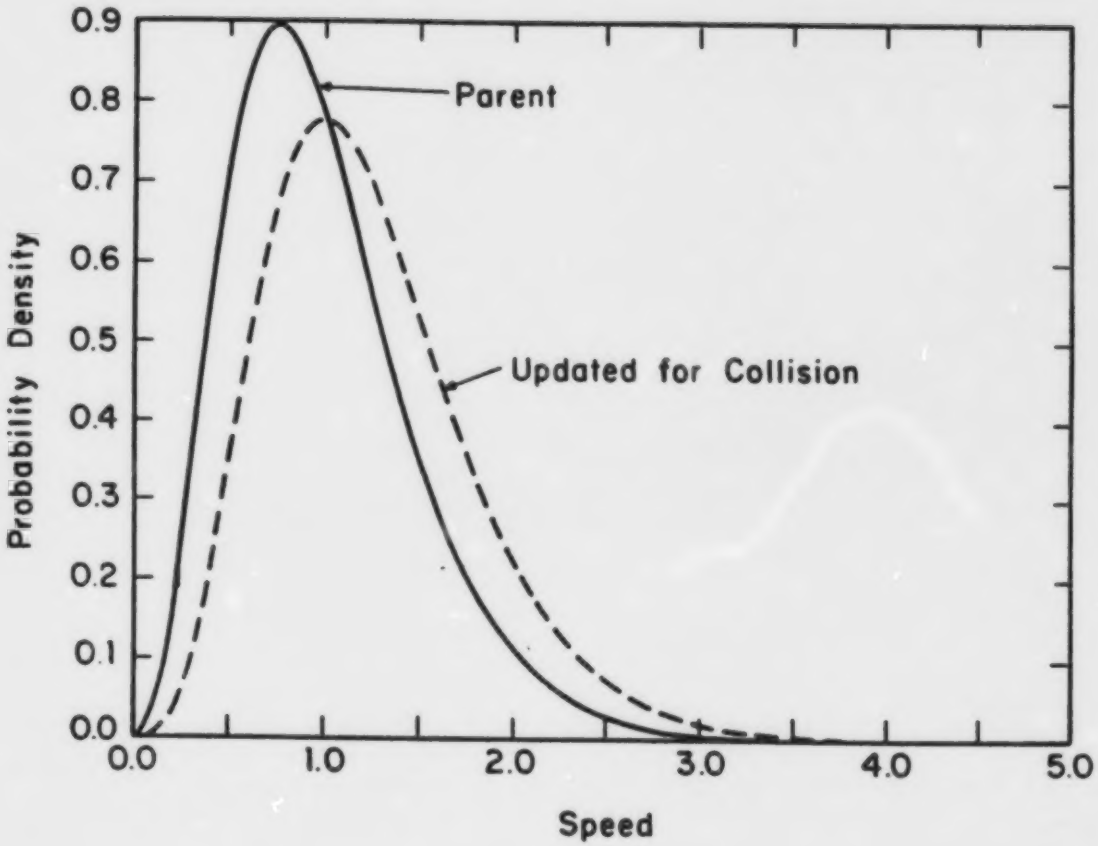


Figure 2.5 Gamma probability density function for ice speed and updated distribution conditional on collision

# 3. MODELLING OF THE ENVIRONMENT

## 3.1 Overview

The implementation of the statistical methodology described in the preceding chapter is carried out according to the flow chart shown in Figure 3.1. First, for the location under consideration, the scenarios are defined. Generally the sets (FL, MP, MS) or (FP, MP, MS) will cover most situations, and the important groups can be reduced to (FL, MS) and (MP, MS) for the more severe interactions, i.e. ignoring the scenarios that occur briefly or do not cause the critical loads.

The next step is to define the season boundaries: these will vary from year to year and are random. For operational decision-making, for instance in determining the probability of open water for transportation on a given date or the length of the open water season (treated as a random quantity), the year to year variation is important. This is also the case if the extreme load over a short period of time is required, as against the maximum for a long period of time, in which case a mean season length is more appropriate.

Given the season length, the expected number of arrivals of events of importance is obtained. The key events are as follows:

(i) Landfast ice - storms above a specified threshold

- breakoff events

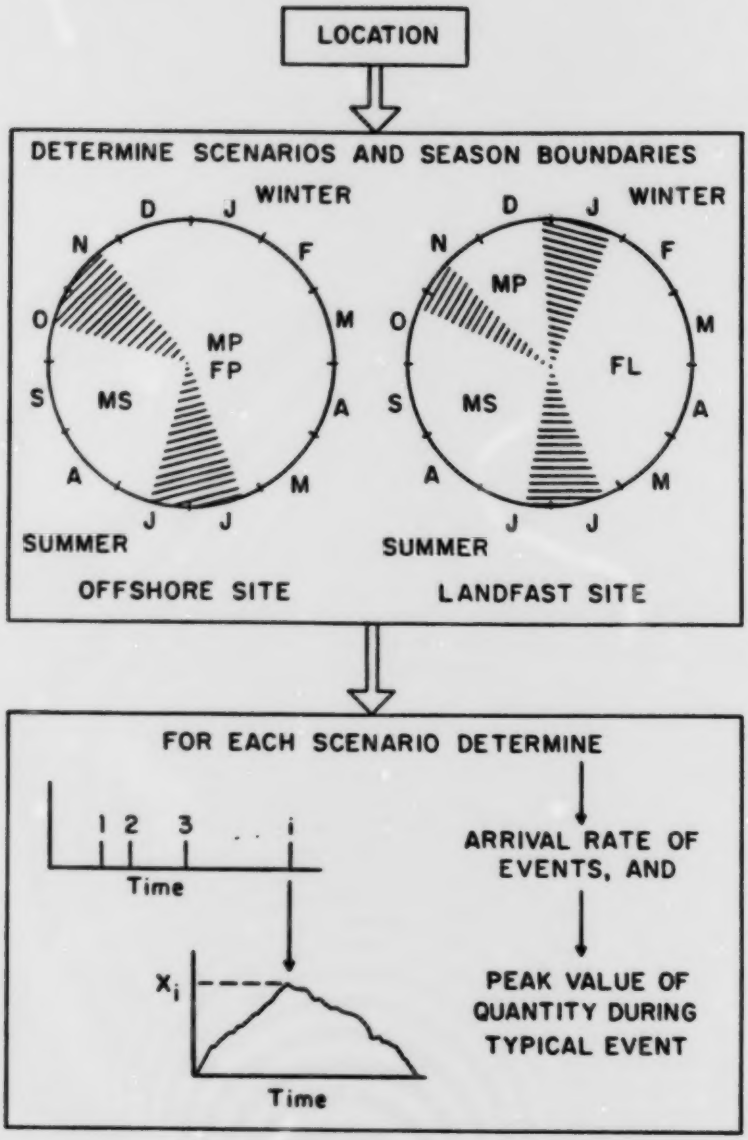


Figure 3.1 Statistical methodology for determining environmental events that result in peak loads

(ii) Pack ice (first year) - storms or ice velocity above a specified threshold

(iii) Multiyear ice - arrival at the structure location and subsequent interaction.

The events occur randomly in time with a certain arrival rate $\lambda$; $\lambda$ can be a function of time, or a constant. For the case where $\lambda = \lambda(t)$, the expected number of arrivals is $\nu = \int\lambda(t)dt$ where the integral is taken over the season length, which may itself be random.

Given an event, there are several quantities of interest: examples are the peak load during the event, the ice thickness, the peak ice velocity, multiyear floe size or maximum ridge thickness in a floe. The series of quantities of interest ($X_1$, $X_2$, ..., $X_i$, ...$X_N$) therefore corresponds to the series of events ($E_1$, $E_2$, ..., $E_i$, ...$E_N$) (see Figure 3.1). As noted above, N can be random. The series of ($X_i$), i=1, ..., N is subjected to extremal analysis, i.e. the quantity $Z = \max(X_i)$ is studied.

The question of ice loads is the final end product that is of concern. The following section puts this briefly into the context of the other environmental parameters.

## 3.2 Ice Load Modelling

An appropriate relationship for the load y transferred from ice to a structure with vertical sides is the following:

$$y = \bar{p}\, w\, h, \qquad (3.1)$$

where $\bar{p}$ = mean ice pressure, w = width of the structure and h, as before, = ice thickness. It is assumed that $\bar{p}$ takes into account the shape of the structure (e.g. polygonal as against circular shape in plan) or contact effects between the structure and the ice.

The approach embodied in the preceding paragraph is intended to provide a simple vehicle for communication between environmental researchers and engineers interested in the estimation of ice loads. A detailed analysis of ice-structure interaction would involve quite complex time-stepping algorithms; conical or sloping structures involve a different type of icebreaking (flexural failure). Nevertheless, the ingredients remain the same: measures of ice thickness dimensions and ice strength are required to obtain design loads.

Pursuing the analysis using equation (3.1), a useful concept is the cutoff stress method (Walden et al., 1987). This is illustrated in Figure 3.2. It is clear that the velocity of interaction is important for two reasons: (i) the effective ice pressure $\bar{p}$ and hence the load, is strongly dependent on velocity in the creep regime ($v<v_c$); (ii) while the value of $\bar{p}$ is less dependent on velocity for $v>v_c$, it is important to know whether v is less than or greater than $v_c$. Also, the dynamics of the situation (ice-induced vibration) is related to velocity.

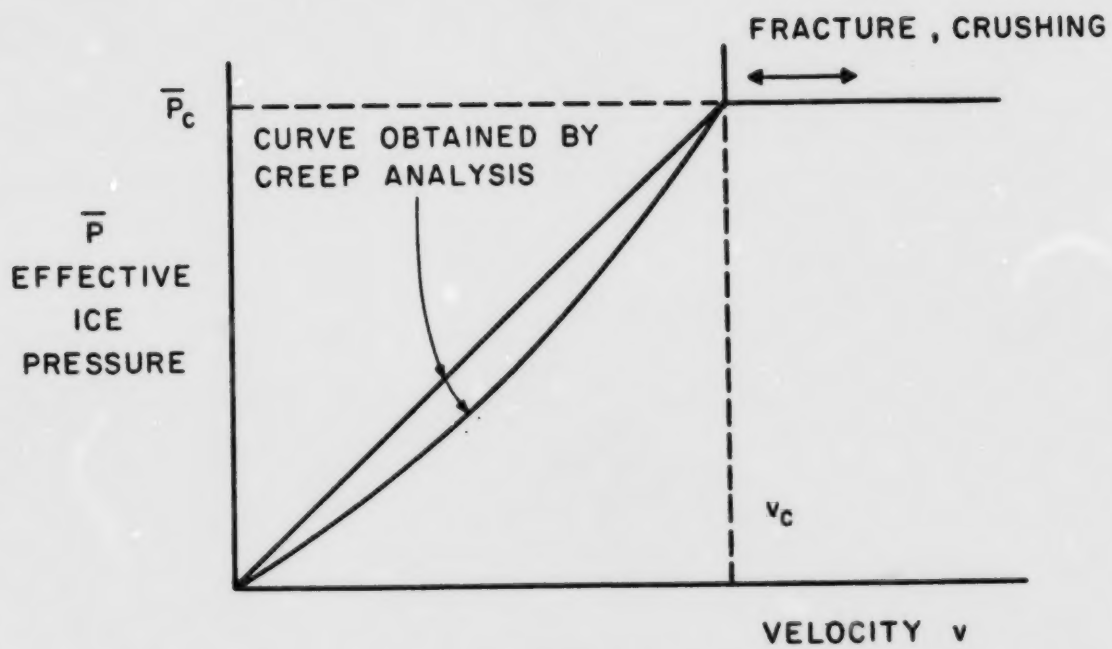


Figure 3.2 Cut-off stress approach

## 3.3 Season Lengths

Rather than calculating ice conditions on a daily or weekly basis, it is sufficient to consider average conditions over only a few seasons during the year. In defining the transition between seasons, the ultimate goal is the effect of this choice on the ice-structure interaction problem. The choice of seasons is not arbitrary and should reflect natural changes in ice conditions. If natural boundaries such as freeze up and break up are used, environmental parameters for design will not be sensitive to small variations of a week or so in the definition of the season boundaries. The length of the exposure to each of the interaction scenarios defined in Section 1.2 is of importance; this will dictate the time t in the calculation of the expected number of arrivals of a particular event $\nu = \bar{\lambda}t$ where $\bar{\lambda}$ is the mean arrival rate.

The first consideration for defining break up and freeze up is the change in total ice concentrations. This strategy is outlined by the following simple rules and summarized in Figure 3.3.

Breakup:

Start — $C \leq 8/10$ and does not return to 10/10 until after the finish of breakup. The cutoff value of 8/10 was chosen so that the opening of isolated leads would not incorrectly signal the end of the landfast season.

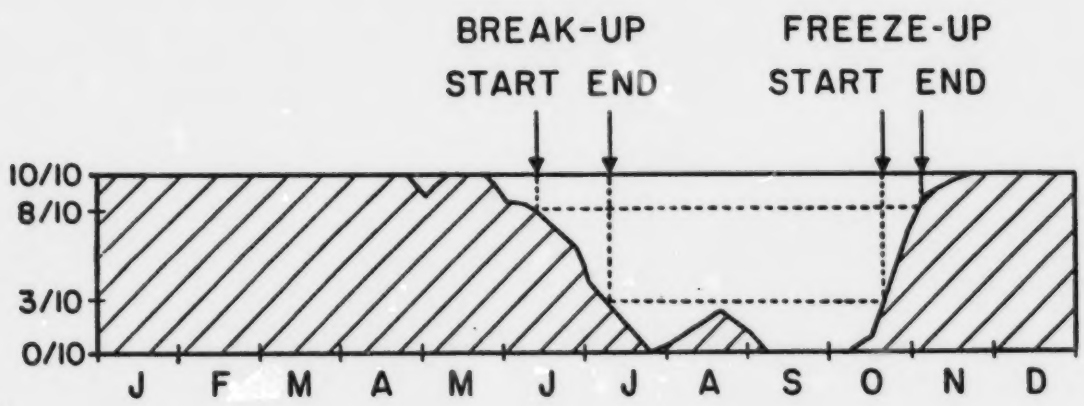


Figure 3.3 Ice concentrations used as guidelines for establishing break up and freeze up dates

Finish — $C \leq 3/10$ and is not exceeded for two weeks. If this concentration is not exceeded for two weeks, any large floes are assumed to have broken up and subsequent ice is assumed to be the result of pack ice intrusions.

Freeze up:

Start — Week after last week that coverage $\leq 1/10$. The new thin ice may be broken up by the wind resulting in initial low concentrations but once the presence of ice becomes uninterrupted until spring, freeze-up is assumed to have started.

Finish — When coverage reaches $\geq 8/10$. Once coverage reaches 8/10, it nearly always remains so for the duration of the winter.

Ice thickness can also be a determining factor in the establishment of season boundaries; it is a constraint that must be satisfied before freeze up can occur. The presence of ice is not important when it is less than a minimum thickness. Experience dictates that, until a 30 cm thickness is reached, ice structure interaction scenarios are unaffected by the presence of first year ice. Below this thickness, pieces of the ice tend to slide over one another, a process known as rafting, and the ice will not transmit any significant horizontal forces. One way of accounting for this is to use the coverage of ice of a given thickness (e.g. white ice) in the above distributions; an alternate approach using ice growth information is now presented.

During the course of the winter in the Beaufort Sea, landfast ice grows outward from shore and may envelop the offshore structure. The end of the landfast ice season was assumed to occur at the breakup date. The start of the landfast ice season was defined by whether the site actually became landfast during the year and the date at which this occurred.

The above information can be summarized in Figure 3.1. Two winter scenarios are proposed: an offshore site that is seldom or never enclosed by landfast ice (e.g. Amauligak) and a brief pack ice season followed by landfast conditions (e.g. Kaubvik).

The above rules governing the choice of season boundaries have been summarized in Table 3.2. The variance in the mean breakup date was calculated from the average variance of the start and end dates. The variance in the freeze up date is the sum of the variance from the ice concentration criterion marking the end of freeze up and the variance of the time to reach 30 cm ice thickness, given that total ice concentration has reached 8/10. The variance in the length of the seasons is simply the sum of the values for break up and freeze up, assuming the independence of these two events.

## 3.4 First Year Ice Thickness

First year ice thickness is a key parameter for design. It is a linear scaling factor on first year pack ice and landfast ice loads, and influences the motion of the first year and multiyear pack ice. In this section, an

Table 3.2 Rules governing the definition of season boundaries for the Beaufort Sea

| Boundary | Definition | Specification |
|---|---|---|
| freeze up | The date at which 8/10 coverage of ice 30 cm or greater is reached | Coverage of all ice is obtained from the digital data bases; freeze up date follows this by 10 days to allow for 30 cm ice growth |
| start of landfast ice season | The date that the site is enveloped in landfast ice (note that there is an annual probability that landfast ice is indeed present at the site) | Estimated from maps of landfast ice extent |
| breakup | The average of (i) the date at which 8/10 coverage is reached and never exceeded and (ii) the date at which 3/10 coverage is reached and not exceeded for 2 consecutive weeks | Determined from the coverage of all ice ice in the digital data bases |

approach is presented for obtaining the seasonal distribution of ice thickness and the maximum annual values based on local air temperatures.

Although the AES ice charts obtained from aerial reconnaissance contain the stage of development of the ice cover, this information is not accurate for determining ice thickness, particularly for older first year ice. Ice thickness has been measured directly at various locations throughout the Canadian Arctic (e.g. Richardson and Burns, 1975; Parker, 1987). In the latter reference, ice thickness measured at Kugmallit Bay near Tuktoyaktuk was reported for 1971 to 1977 (Figure 3.4a). Longer records were available from Cape Parry and at Thesiger Bay near Sachs Harbour but average maximum ice thickness was less, neglecting the bias introduced by the different periods of record. The ice thickness time series can be extended for Kugmallit Bay using the relation between thickness and accumulated freezing degree days in Figure 3.4b reproduced from Parker (1987). The latter approach is investigated in this section.

Assuming a constant vertical temperature gradient in the ice, heat loss through conduction results in a linear relation between the square of ice thickness and accumulated freezing degree days. In practice, this is accurate as demonstrated by Parker (1987) except that there is an offset in the linear relation since some accumulation of freezing temperatures is required before any ice growth occurs. For Kugmallit Bay, the resulting relation is

$$h^2 = -0.242 + 0.000936\ AFDD$$

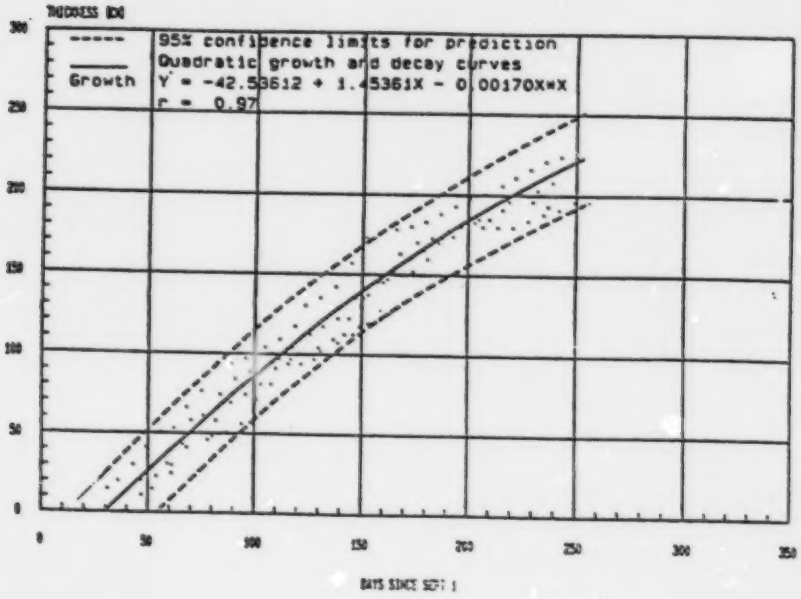


(a)

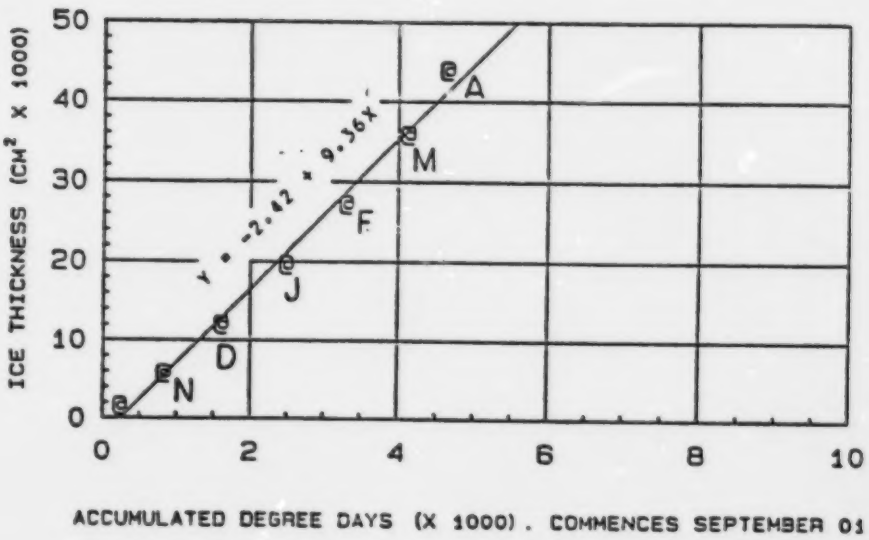


COEFFICIENT OF CORRELATION IS .884727

(b)

Figure 3.4 Landfast ice thickness at Kugmallit Bay near Tuktoyaktuk (1971-1977)
(a) ice thickness as a function of date, and
(b) relation between ice thickness and freezing degree days (from Parker, 1987)

where h is the ice thickness in metres and AFDD is the number of accumulated freezing degree days. Ice thickness is sensitive to the offset constant at the beginning of the season but the effect is negligible on ice thicknesses that approach 2 m late in the winter.

The above relation is only correct for ice growth up to the maximum ice thickness in a given year. If the entire seasonal distribution is required, it is necessary to account for the decay in thickness in the spring. Solar radiation plays a larger part during this period, nevertheless the decay can be approximated by applying a rate of 10 times the growth rate to accumulated melting degree days. Fortunately, breakup of the landfast ice occurs within two months of the date of maximum thickness and the overall thickness distribution is not sensitive to the assumed decay rate.

## 3.5 Wind Induced Ice Drift

Ice loads on structures arise from movement of ice; in the Beaufort Sea, wind is the predominant driving force on the ice. The drift speed of pack ice has been identified as having a significant contribution to ice impact with fixed offshore structures because of its influence on the arrival rate and impact velocity of multiyear floes. Multiyear floes generally move at the same rate as neighbouring first year ice; this means that the motion of multiyear and firstyear floes can be considered in the same way.

The motion of Arctic pack ice has been studied extensively as it varies

spatially (e.g. Colony and Thorndike, 1984; McKenna, 1986) and as it is influenced by winds (e.g. Overland, 1985; Thorndike and Colony, 1982) and by the ocean (e.g. McPhee, 1986). Particularly over time scales of hours to a few days, there is a strong correlation of ice motion with wind (Figure 3.5). Note however the influence of shore on the onshore motion.

Historically, ice motion has been poorly documented because of the difficulty in its measurement. Only recently has it been possible to determine ice velocity from data buoys deployed on the ice and from remotely sensed imagery. Historical wind records are extensive and therefore the link between wind and ice motion can be used to augment ice velocity distributions. Winds contained in the AES data bases are used in the following analysis. Ice concentrations are obtained from the AES Regional ice data and the SIGRID data accessed via CRISP.

In summer, ice floes float freely and the ice velocity can be calculated from the balance of the applied wind stress and the water stress. A significant proportion of the variance in the motion is accounted for by the wind; there is no consistent ocean circulation independent of the wind that drives the ice pack, except during major storm events. The consideration of storm induced currents is beyond the scope of this report. The ice speed distribution needs to be corrected in these cases.

The situation is complicated in winter when first year ice concentrations approach 10/10. The ice pack motion is wind driven as long as there are refrozen leads of weaker ice surrounding the thicker first year

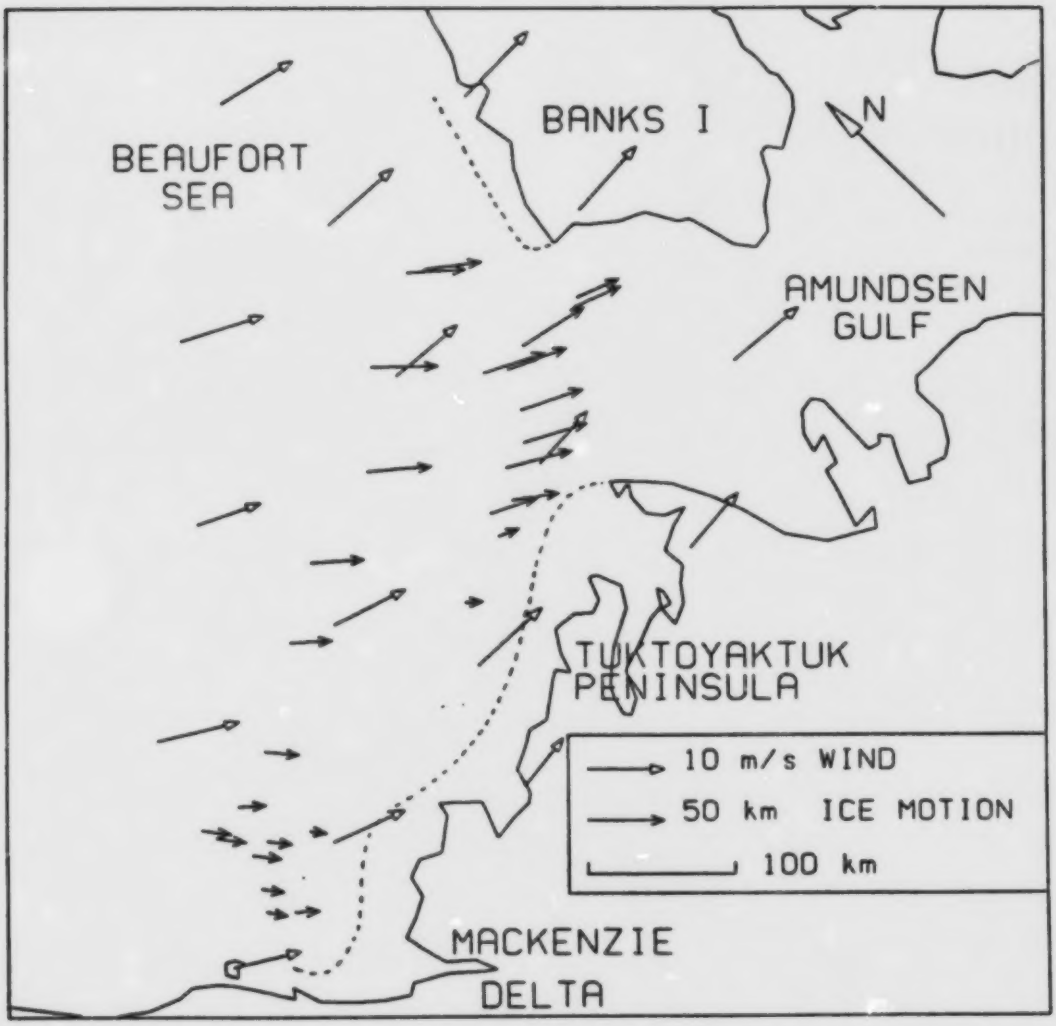


**Figure 3.5** Beaufort sea average wind and ice motion for February 28th. to March 3rd. 1983. The dashed line denotes the edge of the landfast ice.

ice. In the Beaufort Sea, sites of interest are typically within 75 km of shore or the outer limit of the landfast ice. When consistent onshore winds are present, the ice pack consolidates and force is transmitted from shore or the edge of the landfast ice, reducing the ice velocity. The transition between motion and a stationary state tends to be abrupt, taking place within only a few hours.

Although complex numerical models exist to predict ice pack motion (e.g. Coon et al., 1980; Hibler, 1979; Thomson et al., 1987), the basic features of the ice speed can be captured in a one dimensional model (e.g. McKenna et al., 1983). This model has the form

$$\frac{v}{v^*} = g \tag{3.3}$$

where the ice velocity is denoted by v, the free drift velocity in the absence of any resistance is given by $v^*$ and the coefficient g is a velocity scaling factor ($0 \leq g \leq 1$). The scaling factor is equal to 1 for ice concentrations less than 10/10 and for offshore motion. When the ice concentration is 10/10 and when onshore motion persists causing a consolidation of the ice pack, the factor is 0. Definitions of the free drift ice velocity and of the velocity scaling factor are presented in the following paragraphs.

Considering the steady state equations of motion for a floating ice pack, the effect of coriolis acceleration on ice speed is insignificant

except for small wind speeds. Ice speed can therefore be determined from the one dimensional relation

$$\rho_a c_a v_a^2 - \rho_w c_w v^2 + \frac{\partial \sigma}{\partial x} = 0 \qquad (3.4)$$

where $\rho_a$ and $\rho_w$ are the densities of the air and water respectively, $c_a$ and $c_w$ are the corresponding drag coefficients, $v_a$ is the surface wind speed, v is the ice speed, $\sigma$ is the horizontal stress integrated through the thickness of the ice pack and x is distance. The free drift ice speed is

$$v^* = \left(\frac{\rho_a c_a}{\rho_w c_w}\right)^{1/2} v_a \qquad (3.5)$$

which is the maximum ice speed calculated from (3.4) in the absence of the ice stress term.

Referring to Figure 3.6, the ice pack is free at x=0, fixed at some distance, $\ell$, and is driven by the wind velocity $v_a$, over a stationary ocean. This relation can be simplified by making some assumptions for the ice constitutive behaviour that influence the stress, $\sigma$. Idealizing the process of ridge building, the deformation of the ice is assumed to be rate independent and governed by a limit stress, $p^*$. In this case, the maximum value that the stress term can achieve is

$$\frac{\partial \sigma}{\partial x} = -\frac{p^*}{\ell} \quad , \qquad (3.6)$$

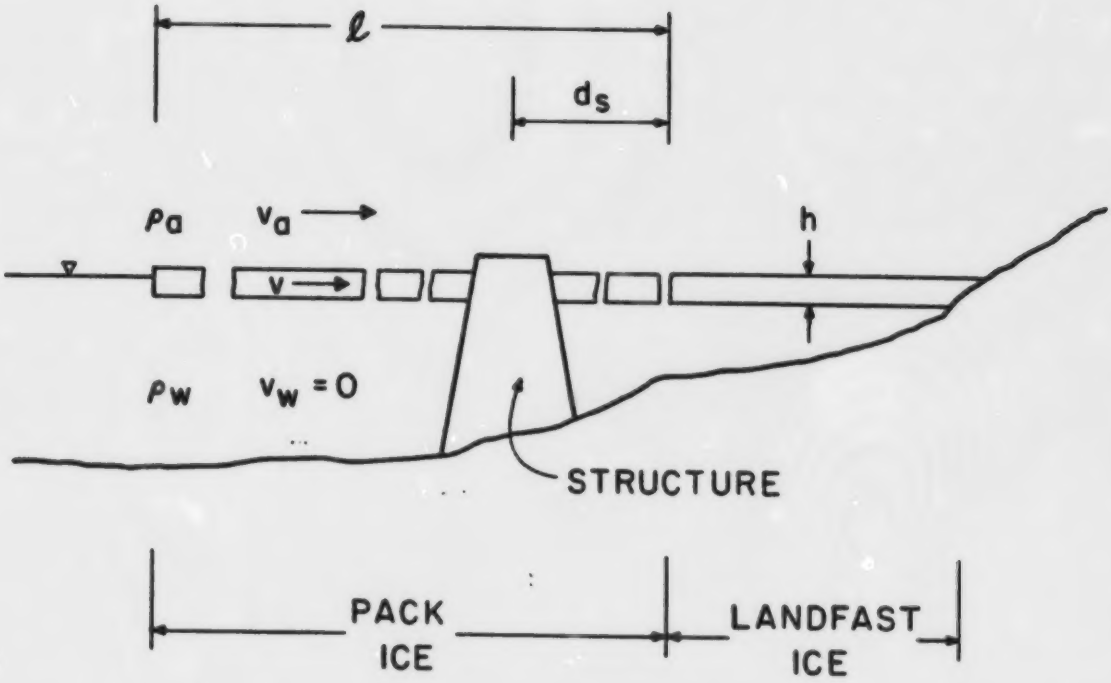


Figure 3.6 Cross section through the ice pack annotated with the motion model parameters

where $\ell$ is the horizontal extent or fetch length of the ice pack. Making this substitution in the equations of motion and recalling (3.3), the velocity reduction factor is given by

$$g = \begin{cases} (1 - \frac{p^*}{p})^{1/2} & p > p^* \\ 0 & p \leq p^* \end{cases} \tag{3.7}$$

The applied force on the ice pack due to the wind is

$$p = \rho_a c_a v_a^2 \ell \, . \tag{3.8}$$

As long as the applied force to the ice pack does not exceed the ice resistance, no motion can occur. For loads, p, greater than the resistance, $p^*$, ice velocities up to a maximum of the free drift value are possible.

Both the ice extent and the ice resistance depend on the recent onshore motion of the pack ice. Onshore motion may either be unimpeded or impeded as shown in Figure 3.7, while offshore motion is generally unimpeded. Onshore drift is estimated from

$$v' = v \cos \theta \tag{3.9}$$

where $\theta$ is the difference between the drift direction and the outward normal direction to shore. The drift direction can be obtained from wind direction corrected for coriolis and local effects. The net onshore displacement is

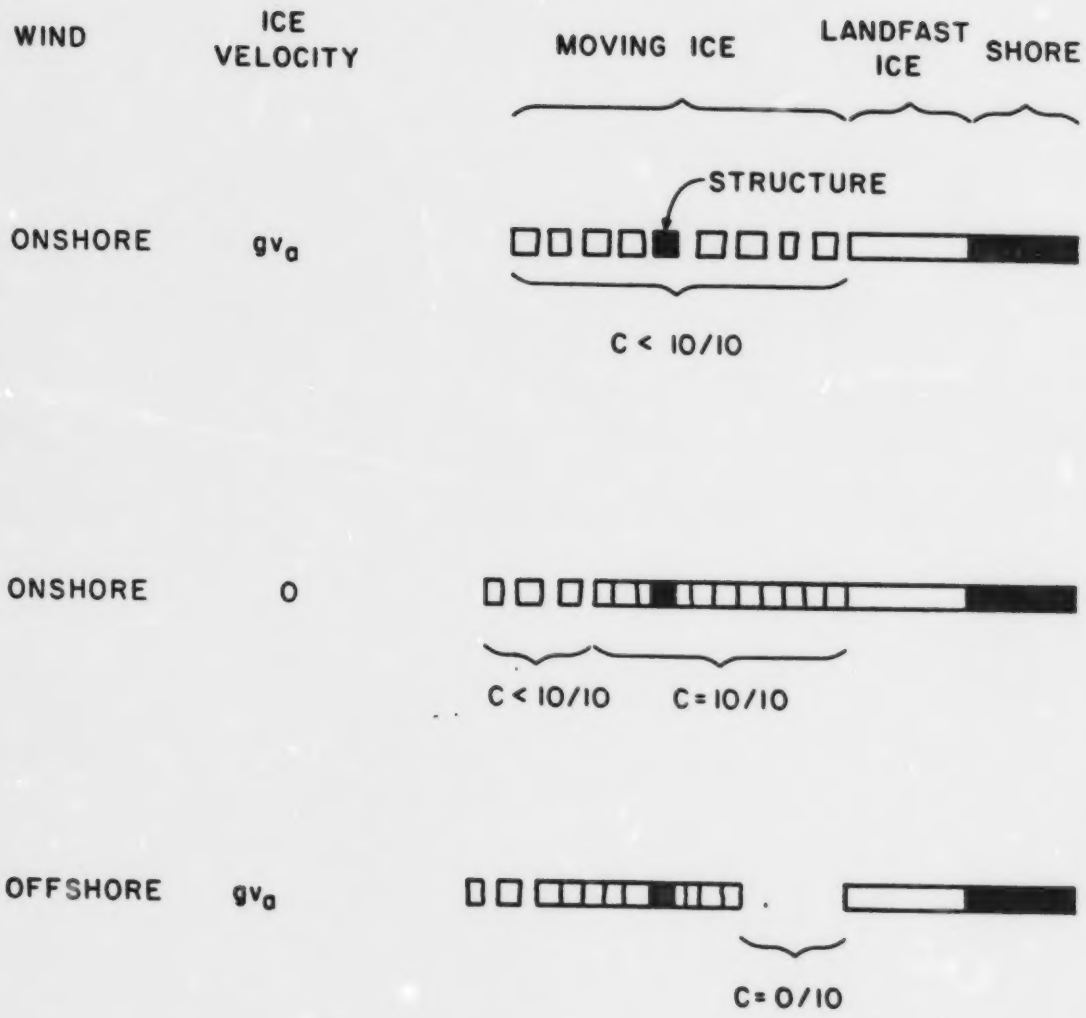


Figure 3.7 Schematic of nearshore ice drift illustrating the velocity scaling factor

then given by

$$d = \int v' \, dt \tag{3.10}$$

where the integral is calculated over recent time. As long as the motion is offshore ($v'<0$) or there is an open flaw lead adjacent to shore ($d<0$), there is no velocity reduction and $g=1$. The flaw lead is only allowed to open by a specified maximum value $d_s$, therefore if $d < -d_s$, then $d = -d_s$.

The ice velocity is reduced for onshore motion according to the applied pressure p and the ice resistance $p^*$. For an ice concentration of 10/10, the fetch length in (3.6) is a fixed maximum value ($\ell = d_f$). When the iceconcentration is less than 10/10, the applied pressure is only non zero when $d > 0$ ( $\ell = d/c$; to a maximum of $d_f$).

The ice resistance is calculated as

$$p^* = (c^* / c_m) \, q \, h \tag{3.11}$$

where h is the ice thickness and q is a constant. The concentration, $c^*$, must be positive and not exceed the concentration of weak ice present in 10/10 concentration ice cover, denoted $c_m$. It is calculated from

$$c^* = x / d_s - (1 - c). \tag{3.12}$$

The parameter $d_s$ is the distance of the site from shore.

The ice speed (equation 3.3) is a function of the uncertainty in the principal driving force, the wind, and in the parameters described above. In the following assumption, the variability due to these two effects is isolated. The coefficient of variation for the ice velocity is expressed as

$$V_v = \frac{\sigma_v}{\bar{v}} , \tag{3.13}$$

where $\sigma_v$ is the standard deviation and $\bar{v}$ is the mean. The variance of velocity as a function of the other parameters in (3.3) was calculated using a truncated Taylor series expansion of ice velocity about the mean

$$\sigma_v^2 = (\frac{\partial v}{\partial v^*})^2 \sigma_{v^*}^2 + (\frac{\partial v}{\partial g})^2 \sigma_g^2 . \tag{3.14}$$

resulting in

$$V^2_v = V^2_{v^*} + V^2_g \tag{3.15}$$

Similarly, we obtain

$$V^2_{v^*} = \frac{1}{4} (V^2_{c_a} + V^2_{c_w}) + V^2_{v_a} \tag{3.16}$$

and

$$V^2_{g} = \frac{1}{2(p/p^* - 1)} \quad (V^2_{p} + V^2_{p^*}) \tag{3.17}$$

First of all, for low ice strength ($p^* \ll p$), $g=1$, $V^2_{g} = 0$ and equation (3.15) implies that the variability of ice motion is caused entirely by the variability in the free drift velocity (e.g. (3.16)). For high strength ($p^* \approx p$), $V^2_{v}$ approaches infinity, but the magnitude of v is itself approaching zero since $g=0$ and its contribution is not significant to the calculation of mean ice velocities for design.

Note that (3.15) assumes independence between $v^*$ and g. This is reasonable from the above argument since only one of the terms will dominate in any given situation. The velocity scaling factor g is most sensitive to the accumulated onshore motion and to the wind direction, but not necessarily to the ice speed. Independence between p and $p^*$ is also a requirement for (3.16). Experience, however, has shown that when $p^*$ is not zero it nearly always exceeds p.

An important pattern emerges in the ice drift model. When there is no force transmitted from shore to the pack ice, the variability in ice velocity is entirely due to (3.16) in which the variability due to wind speed dominates. When there is interaction with the shore, the ice velocity is zero. The relative time under which these two opposing situations occur can be related directly to when $p^* \neq 0$.

# 4. DURATION OF SCENARIOS FROM AES DATA

## 4.1 Data Sources

Ice seasons were established for the Amauligak and Kaubvik sites according to the scenarios defined in section 1.2. Season boundaries were required for determining the distributions of ice speed and ice thickness; the season lengths were necessary for computing arrival rates.

Two sources of data were identified to assist with the estimation of breakup and freeze up dates; these were the SIGRID and AES Regional digitized data bases. Weekly ice concentrations for Amauligak obtained are illustrated in Figure 4.1 for the SIGRID data and in Figure 4.2 for the AES Regional data. There is considerable variation in ice concentration during break up; this is more the result of wind conditions than due to ice growth and decay. In most cases, the break up period is significantly longer than freeze up. The Regional data is only available for the summer (typically June to October inclusive) and thus breakup or freeze up can occur outside the collection period. Using only the years of data which span the summer season introduces a bias into the results, giving later average breakup and earlier average freeze up. The SIGRID data base was therefore used for estimating season boundaries.

## 4.2 Ice Concentration Criteria for Season Boundaries

Based on the "all ice" concentration criteria given in Table 3.2, the

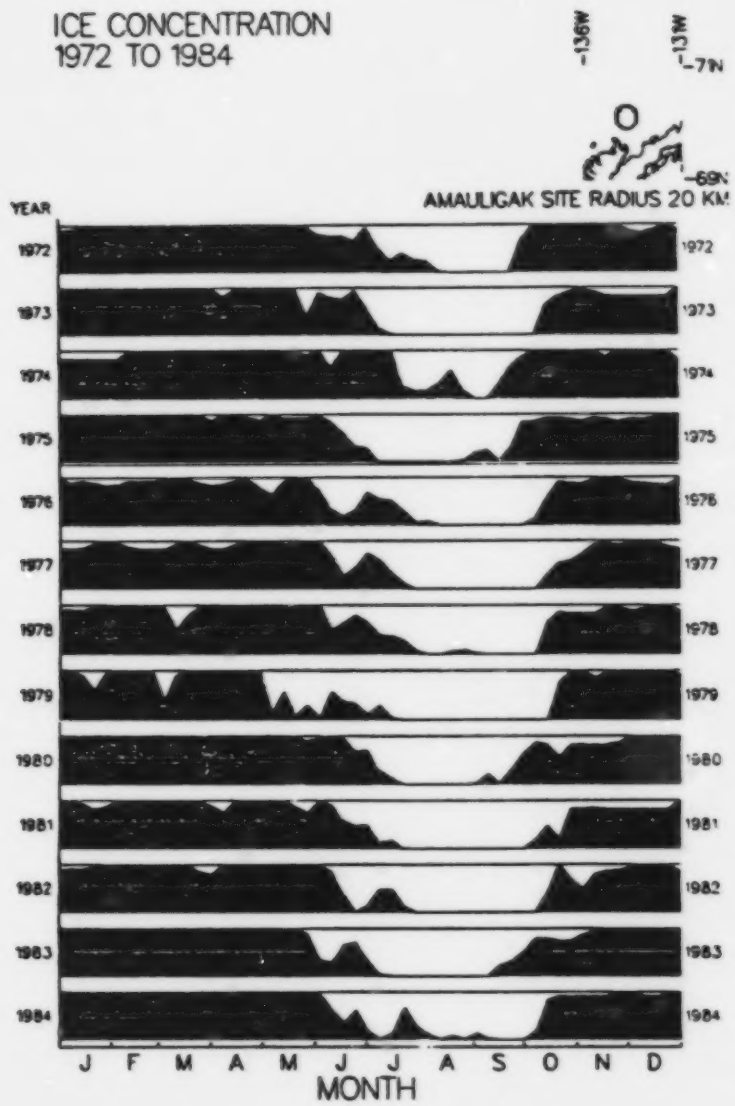


**Figure 4.1 Weekly concentration of all ice at Amauligak from SIGRID data**

ENVIRONMENT CANADA
ATMOSPHERIC ENVIRONMENT CANADIAN CLIMATE CENTRE

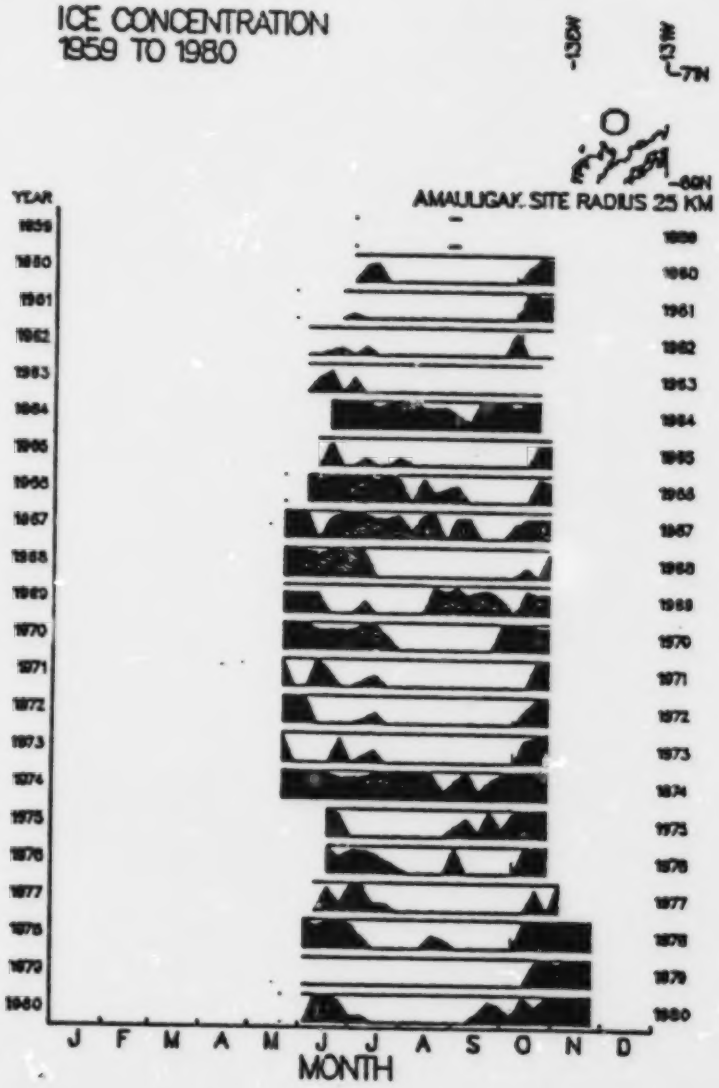


Figure 4.2 Weekly concentration of all ice at Amauligak from AES Regional data

mean dates for breakup and freeze up are given for Amauligak in Table 4.1 and for Kaubvik in Table 4.2. Histograms for the distribution of these dates are given for Amauligak in Figure 4.3 and Kaubvik in Figure 4.4.

## 4.3 Ice Thickness Freeze-up Criterion

Ice concentration is not the only determining factor in establishing season boundaries. As specified in section 3.3, a minimum ice thickness of 30 cm is required, delaying the actual freezeup from the dates given in Tables 4.1 and 4.2. Since no direct measurements of ice thickness have been made at the offshore sites, an indirect approach is required. AES provides measured ice thickness histories at Kugmallit Bay near Tuktoyaktuk, Cape Parry and Thesiger Bay near Sachs Harbour (Parker, 1987). The average date at which a 30 cm thickness is reached varied from October 23rd to November 3rd.

Taking advantage of air temperatures recorded by AES, the relations between ice thickness and freezing degree days calculated by Parker (1987) provide an additional estimate of the start of the winter season. The accumulated freezing degree days corresponding to an ice thickness of 30 cm are 264 at Thesiger Bay, 350 at Kugmallit Bay and 340 at Cape Parry. From the mean Amauligak monthly temperature data, corresponding freeze up dates of November 7th, November 15th and November 15th were estimated. Accounting for a minimum ice thickness requirement of 30 cm, a later date for freeze up than given in Tables 3.1 and 3.2 is recommended. A standard deviation of 3

Table 4.1 Dates defining season boundaries at Amauligak from ice concentration data

| | Data Set | Number of Years | Mean Date | Standard Deviation (days) |
|---|---|---|---|---|
| Start of Breakup | SIGRID | 13 | 18 Jun. | 17 |
| | AES Reg. | 20 | 03 Jul. | 27 |
| End of Breakup | SIGRID | 13 | 12 Jul. | 19 |
| | AES Reg. | 19 | 20 Jul. | 32 |
| Start of Freeze up | SIGRID | 13 | 13 Oct. | 12 |
| | AES.Reg | 18 | 16 Oct. | 20 |
| End of Freeze up | SIGRID | 13 | 23 Oct. | 11 |
| | AES Reg. | 18 | 18 Oct. | 20 |

Table 4.2 Dates defining season boundaries at Kaubvik from ice concentration data

| | Data Set | Number of Years | Mean Date | Standard Deviation (days) |
|---|---|---|---|---|
| Start of Breakup | SIGRID | 13 | 19 Jun. | 19 |
| | AES Reg. | 21 | 29 Jun. | 11 |
| End of Breakup | SIGRID | 13 | 11 Jul. | 21 |
| | AES Reg. | 21 | 29 Jul. | 20 |
| Start of Freeze up | SIGRID | 13 | 14 Oct. | 10 |
| | AES.Reg | 18 | 16 Oct. | 12 |
| End of Freeze up | SIGRID | 13 | 22 Oct. | 10 |
| | AES Reg. | 19 | 17 Oct. | 10 |

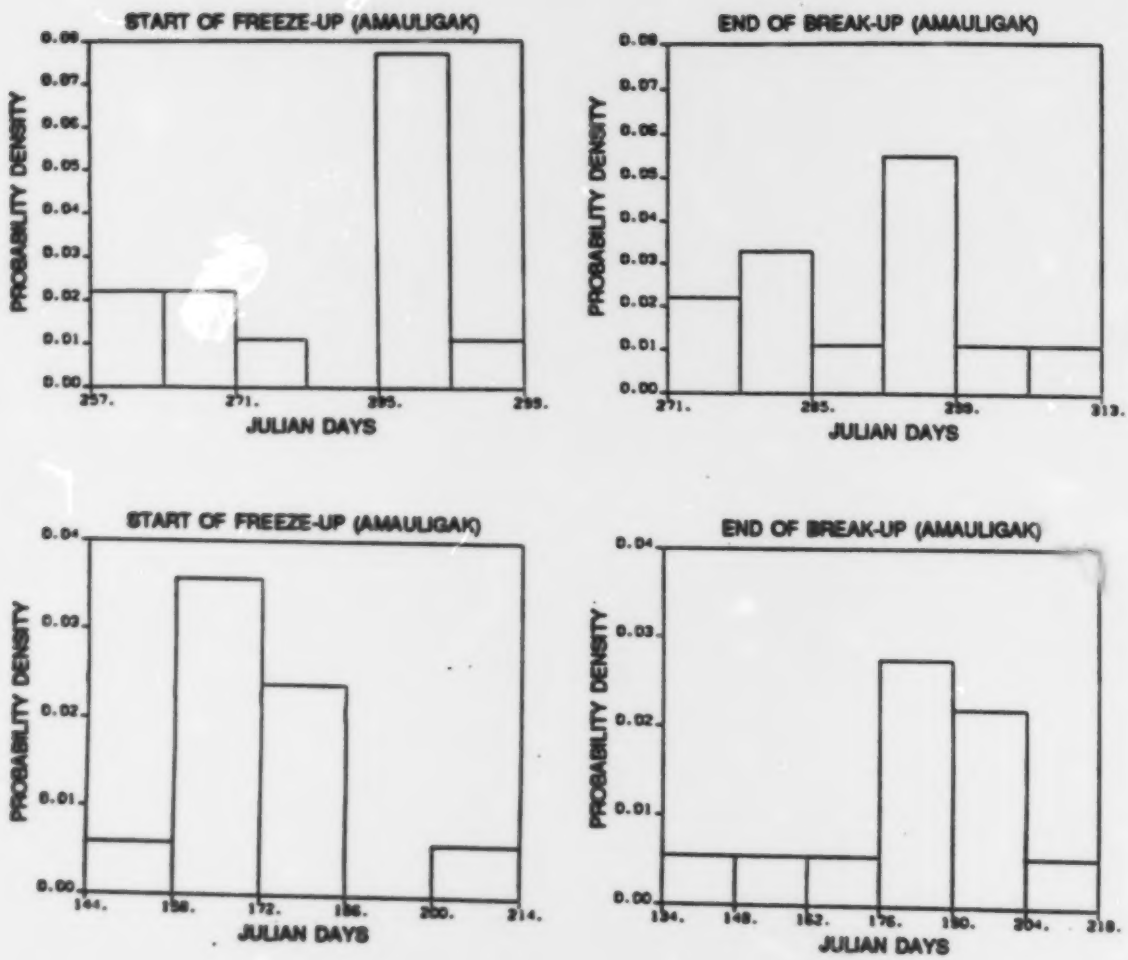


Figure 4.3 Distribution of freeze up and breakup dates based on ice concentration at Amauligak from SIGRID data

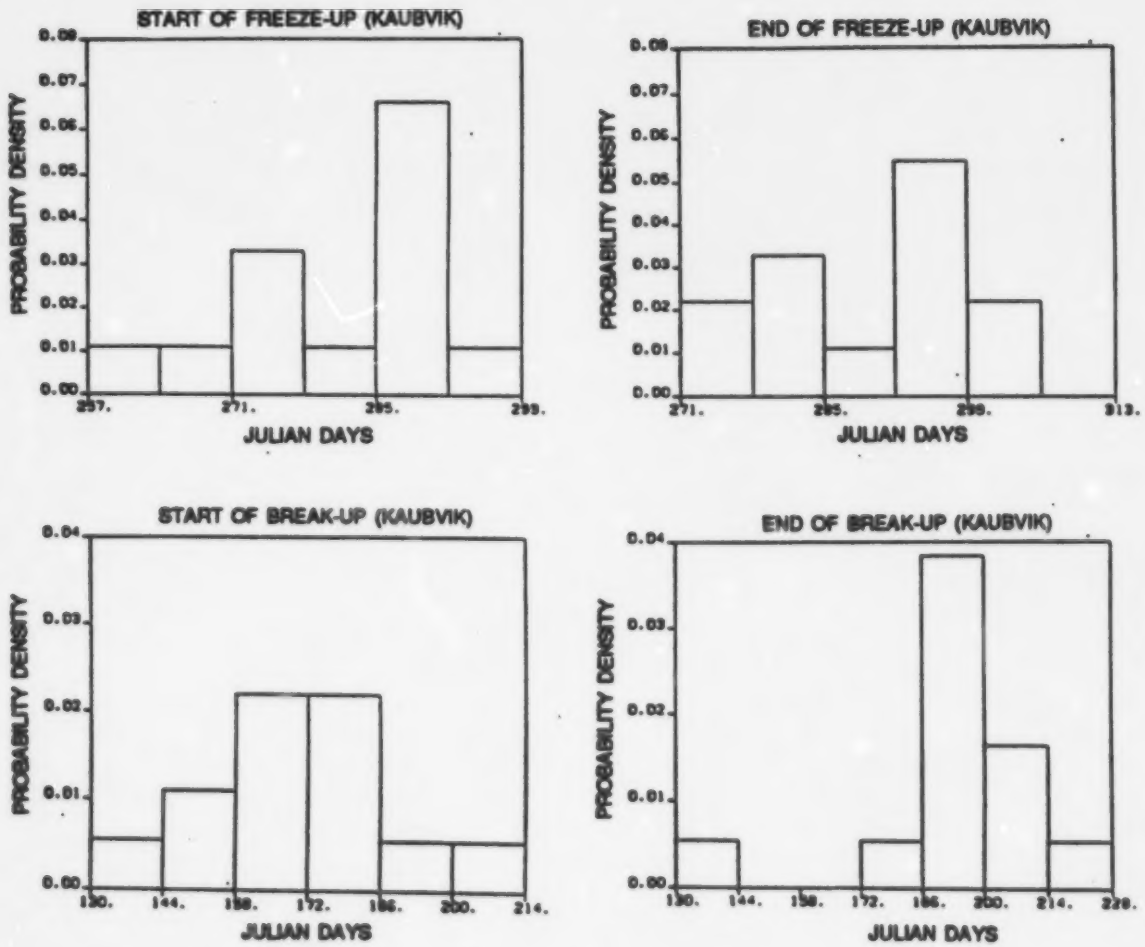


Figure 4.4 Distribution of freeze up and breakup dates based on ice concentration at Kaubvik from AES Regional data

days was estimated for this delay time and the dates of freeze-up were estimated to be November 4th. at Kaubvik and November 5th. at Amauligak.

## 4.4 Landfast Ice Season

Maps of the landfast ice edge were reported by Spedding (1975) and Spedding and Hawkins (1985). This information is summarized for Kaubvik and Amauligak in Table 4.3. Amauligak was landfast at least 11 percent but not more than 33 percent of the year while Kaubvik was landfast 78 percent or 89 percent of the time over the 9 years of data. The corresponding averages of the times before which the sites were landfast were February 5th. and December 25th. Markham (1983) has summarized the minimum, maximum and mean extents of the landfast ice off the Tuktoyaktuk Peninsula for 1960 to 1982. Assuming a normal distribution for the maximum extent, Amauligak was estimated to be landfast 40 percent of the years and Kaubvik about 95 percent of the time. Combining the two data sources, Amauligak was assumed to be landfast 25 percent of years and Kaubvik 90 percent of years. Overall, the landfast ice data were not comprehensive; standard deviations for the dates were estimated to be 30 days.

Examination of the SIGRID data for both Kaubvik and Amauligak showed that there was 10/10 coverage for a substantial portion of most winters. In some cases this indicates a landfast condition, but moving pack ice can have 10/10 concentration, particularly when motion is onshore or the pack ice has not moved for a period of time. Loss of accuracy in the digitization to grid points may also influence these concentrations. At Amauligak, the

Table 4.3 Landfast ice encroachment at Amauligak and Kaubvik (from Spedding, 1975; Spedding and Hawkins, 1985)

| Site | Winter | Landfast (Y/N/?) | Date before which site was landfast |
|---|---|---|---|
| Amauligak | 1972/73 | N | - |
| | 1973/74 | Y | 25 Feb. |
| | 1974/75 | N | - |
| | 1975/76 | N | - |
| | 1976/77 | ? | ? |
| | 1977/78 | N | - |
| | 1979/80 | ? | 15 Jan. |
| | 1980/81 | N | - |
| | 1983/84 | N | - |
| Kaubvik | 1972/73 | Y | ? |
| | 1973/74 | Y | 25 Feb. |
| | 1974/75 | ? | Y:06 Nov, N:30 Mar |
| | 1975/76 | N | - |
| | 1976/77 | Y | ? |
| | 1977/78 | Y | ? |
| | 1979/80 | Y | 27 Dec. |
| | 1980/81 | Y | 7 Jan. |
| | 1983/84 | Y | 10 Oct. |

SIGRID data indicates more than 8 weeks of continuous 10/10 coverage for the winters 1972-73, 1973-74, 1974-75, 1977-78. The SIGRID data also indicates continuous 10/10 coverage for all winters between 1972 and 1978 except 1975-76 and 1976-77 at the Kaubvik site. These results differ from the direct measurements of landfast ice reported in Table 4.3; it was not possible to establish the length of the landfast ice season from the concentration of all ice in the SIGRID and AES Regional data bases.

The end of winter was selected as the mean of the start and end dates of the break up period. This season boundary is a compromise between the start of breakup at which landfast ice is no longer critical and the latter stages when ice velocity and the multiyear impact scenario are no longer influenced by first year ice concentration. Markham (1983) has summarized the breakup of landfast ice in Kugmallit Bay. From 1959 to 1982, the mean date that breakup was initiated was July 2nd., with a standard deviation of 7 days. These results confirm the above choice but may indicate that the breakup date has less scatter than assumed. Markham also noted a consistent relation between accumulated melting degree days and the breakup date. In future, this is another way in which AES time series data can be used for establishing season boundaries.

## 4.5 Season Lengths

For the Amauligak and Kaubvik sites, the season boundaries selected for further analysis are given in Table 4.4 and the corresponding season lengths are found in Table 4.5. If the ice seasons at Amauligak and Kaubvik are

Table 4.4 Season boundaries for Amauligak and Kaubvik

| Site | Feature | Mean Date | Standard Deviation (days) |
|---|---|---|---|
| Amauligak | freeze up | 05 Nov | 14 |
| | start of landfast ice | 05 Feb | 30 |
| | breakup | 30 Jun | 18 |
| Kaubvik | freeze up | 02 Nov | 13 |
| | start of landfast ice | 25 Dec | 30 |
| | breakup | 30 Jun | 20 |

Table 4.5 Summary of season lengths at Amauligak and Kaubvik

| Site | Season | Probability of Occurrence | Scenarios (see sec. 1.2) | Mean Length (days) | Standard Deviation (days) |
|---|---|---|---|---|---|
| Amauligak | Summer | 1 | MS | 128 | 23 |
| | Winter Pack | 0.75 | MP,FP | 237 | 23 |
| | Winter Pack | 0.25 | MP | 92 | 33 |
| | Winter Landfast | 0.25 | FL | 145 | 35 |
| Kaubvik | Summer | 1 | MS | 125 | 24 |
| | Winter Pack | 0.10 | MP,FP | 240 | 24 |
| | Winter Pack | 0.90 | MP | 53 | 33 |
| | Winter Landfast | 0.90 | FL | 187 | 36 |

similar, this is due to their proximity and the result of the spatially averaged ice concentrations from the digital data bases. The significant difference between the two sites is the presence of landfast ice at Kaubvik in approximately 9 of every 10 years, while landfast conditions only occur at Amauligak once in 4 years.

# 5. LANDFAST ICE INTERACTION

## 5.1 Landfast Ice Processes and Loads

As outlined in section 1.2, ice thickness, ice velocity and the frequency of significant motion events can influence the severity of landfast ice loads on structures in the Canadian Beaufort Sea. Landfast ice motion is not a continuous process but a series of discrete events. Although many factors contribute to the events, the wind is the dominant driving force. In this section, AES wind data is used to investigate the cause of landfast ice events and extremal distributions of the corresponding ice velocities are generated. Ice forces can be directly related to the ice thickness; maximum thickness distributions were therefore calculated using the procedure of section 3.3.

For the calculation of extreme landfast ice loads, we require the distribution of the magnitude of the loads and an estimate of how often these occur. The POT or Poisson load event approach described in section 2.2 is directly applicable. First of all, a parent load distribution can be obtained from the recorded distributions of landfast ice velocity and thickness. Extremal load distributions are then computed from equation (2.6). For example, if 11 events are likely to occur on average in one month, then $\nu$ is 66 (assuming a 6 month landfast ice season) for computing the extremal distribution of annual landfast ice loads.

Typically, landfast ice speeds result in strain rates during encounter

events that do not exceed the transition between creep and crushing ice behaviour. A commonly used approach for determining creep loads on vertical structures is the reference stress method (Ponter et al., 1983)

$$y = \phi\ d\ h\ F_{\sigma}[v/d\phi\psi] \tag{5.1}$$

where y is the total force, d is the structure diameter, h is the ice thickness, v is the ice velocity and $F_{\sigma}[\ ]$ is a reference stress value for the bracketed strain rate. The geometrical constants $\phi,\psi$ relate to the aspect ratio and nature of the ice-structure contact. The important point here is that the force y is directly related to the ice thickness and velocity.

## 5.2 Landfast Ice Thickness

Much of the ice growth is dominated by conduction and its rate is therefore reduced with increasing thickness. This was seen in the measured landfast ice thickness at Kugmallit Bay for 1971-1977 summarized by Parker (1987) (see Figure 3.7 of this report). From the Tuktoyaktuk air temperatures for 1972-1984, the thickness distribution was extended by applying the relation between ice growth and freezing degree days developed in section 3.3. The resulting ice thickness distribution is shown in Figure 5.1. This distribution is also distinctly skewed to the larger thickness. The calculated distributions showed a slight sensitivity to the assumed rate of decay in the spring, but breakup occurs before the ice is completely melted, reducing this effect.

The design landfast ice thickness can probably be taken as the maximum value for the 13 years of record without much sacrifice in accuracy. Nevertheless, it is worth looking at the extremal thickness distribution for an increasing number of events illustrated in Figure 5.1. The distribution quickly approaches a density function lumped at the maximum thickness of the parent distribution.

## 5.3 Landfast Ice Events

The AES data bases do not contain any direct measurements of landfast ice motion. Furthermore, no satisfactory model for the prediction of these events has been developed. In this section, the factors influencing such a prediction are outlined and some ideas on the nature of a successful model are outlined.

For design purposes, it is useful to know both the frequency and magnitude of landfast ice movements. The frequency of movements over a prescribed threshold is easier to predict since it can be related to external driving forces; the actual magnitude depends on complex geometrical features that must be measured directly. A model for predicting the occurrence of landfast ice events is therefore the focus of this section.

The potential driving forces for landfast ice movement are:

(i) wind stress applied directly to the landfast ice;

(ii) pack ice pressure acting along the seaward edge of the landfast ice;

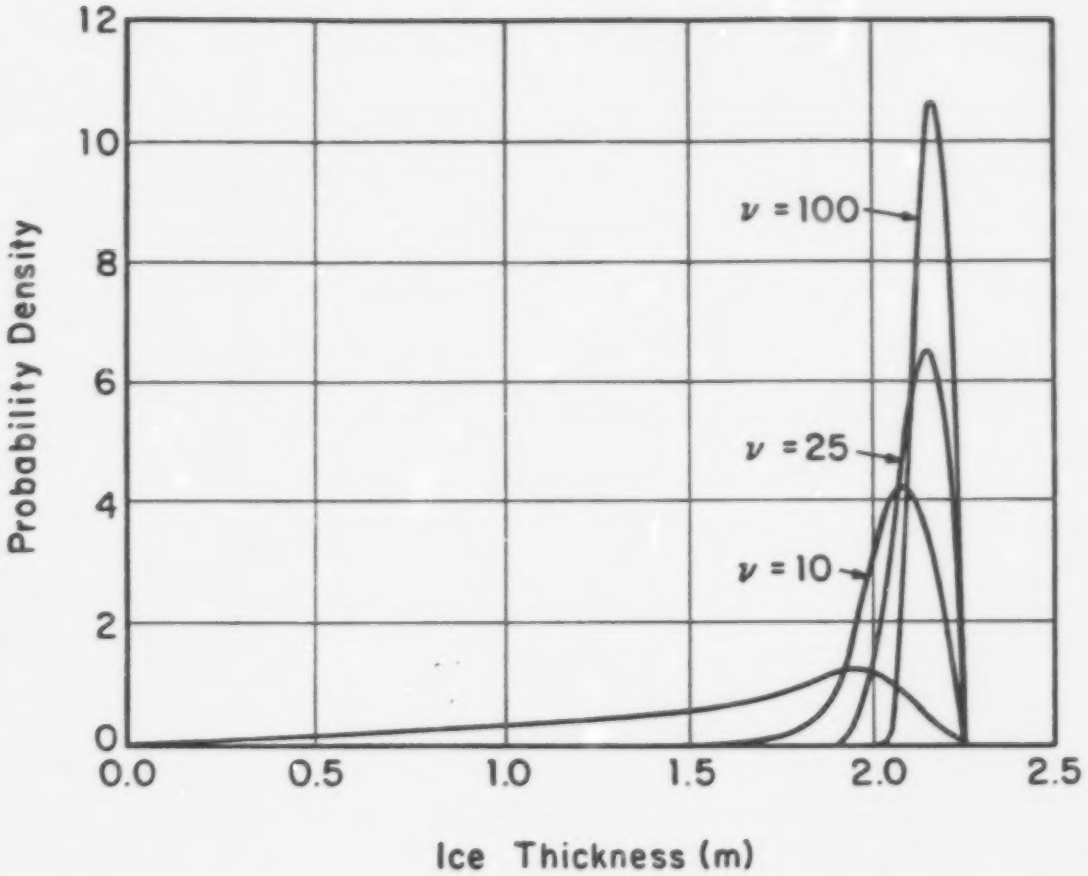


Figure 5.1 Ice thickness distribution calculated from Tuktoyaktuk air temperatures (1972-1984). Extremal distributions are evaluated using equation (2.6)

(iii) tidal forces resulting in small horizontal oscillations of the landfast ice; and

(iv) seasonal and diurnal air temperature fluctuations resulting in expansion or contraction of the ice sheet.

The dominant driving forces for landfast ice movement events are the local wind stress and the pack ice pressure, both of which are wind phenomena. In past studies, attempts to correlate measured wind data with the landfast ice movements have had little success. This is despite a general agreement that wind is the major driving force. A correlation between local winds and measured movement events is complicated by the following factors:

- The presence, direction, and magnitude of movement is affected by the local geography. Movements tend to be larger in deeper water but not necessarily when there are nearby islands or grounded ridges present (Spedding, 1973,1975).
- The wind speed threshold for ice movement is 4.5 m/s to 13 m/s, depending on the wind duration (Spedding, 1975; Agerton et al., 1979).
- The wind duration may be important particularly with regard to pack ice pressure (Tucker et al., 1980).
- The wind direction is important as the ice may be more or less confined in some directions (Spedding, 1973; Agerton et al., 1979).

  The past wind direction is important because a wind can move the ice until all the leeward leads have closed and motion cannot resume until

a change in wind direction occurs (Agerton et al., 1979).

- The magnitude of movements can be governed by the size of leads and weaker regions in the ice sheet rather than the wind speed (Spedding, 1979).
- The wind fetch is important for building of ice stress (Spedding, 1983).
- Increasing ice thickness over the winter leads to smaller ice movements (Spedding, 1977).

Two basic types of landfast ice movement events were observed in the above studies: elastic and permanent (see Figure 5.2). Elastic movements can have magnitudes of up to 15 m (Weeks et al., 1977) and appear as spikes in the ice displacement records. These are typically the result of the application then removal of surface tractions or boundary pressures. Permanent movements appear as ramps in the displacement time series and can have magnitudes of 100 m with rates of 11.7 m/hr (Spedding, 1983). The permanent movements are the result of ridging processes or the opening of cracks.

A preliminary analysis of ice displacement records at Netserk (from Spedding, 1975) and 6 hour average winds at Tuktoyaktuk was used to develop a predictive model for landfast ice events. The ice data consisted of 95 recorded movements from December 1974 to May 1975 at a water depth of 4.3 m, a portion of which is shown in Figure 5.3. Ice movement events were initiated and subsequently terminated by changes in the direction of landfast ice motion. The following features of the data were noted:

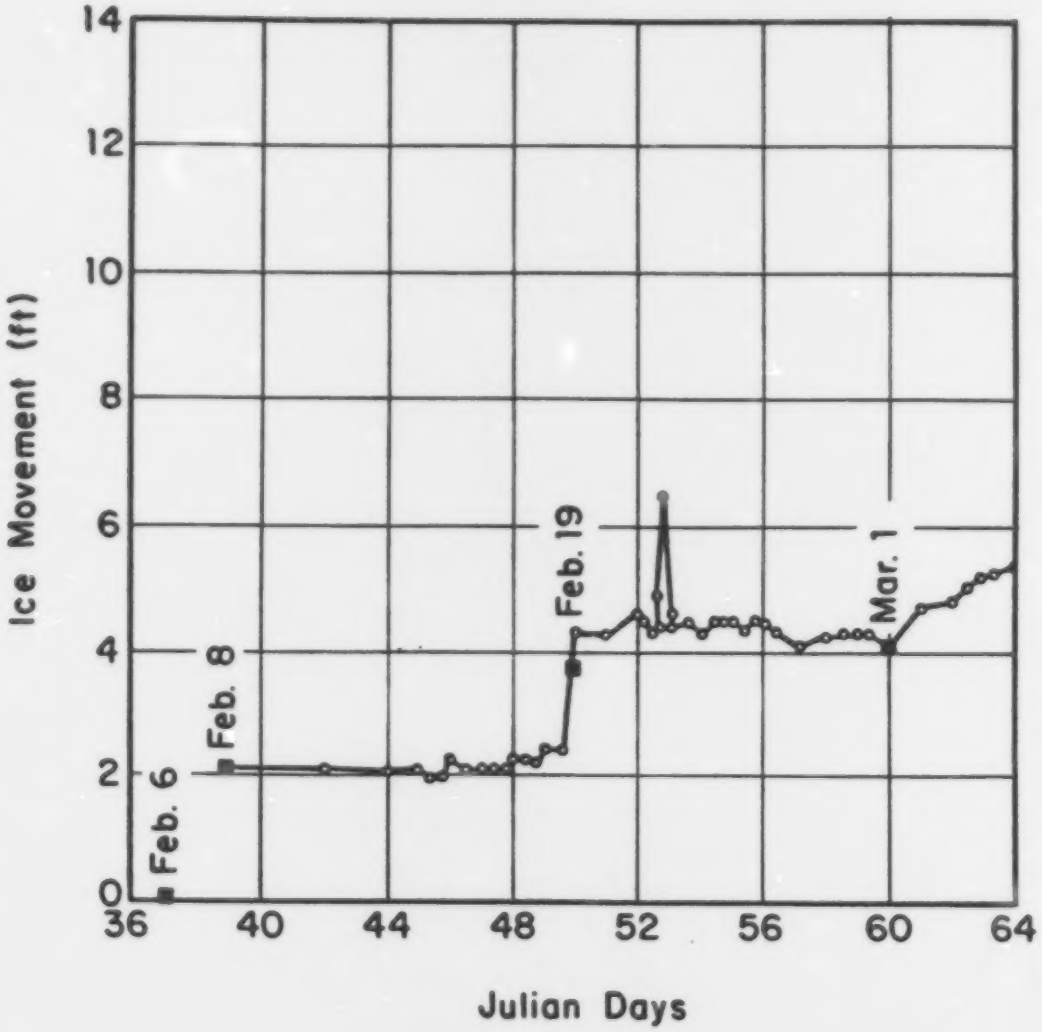


Figure 5.2 Elastic and permanent landfast ice movements (from Spedding et al., 1972)

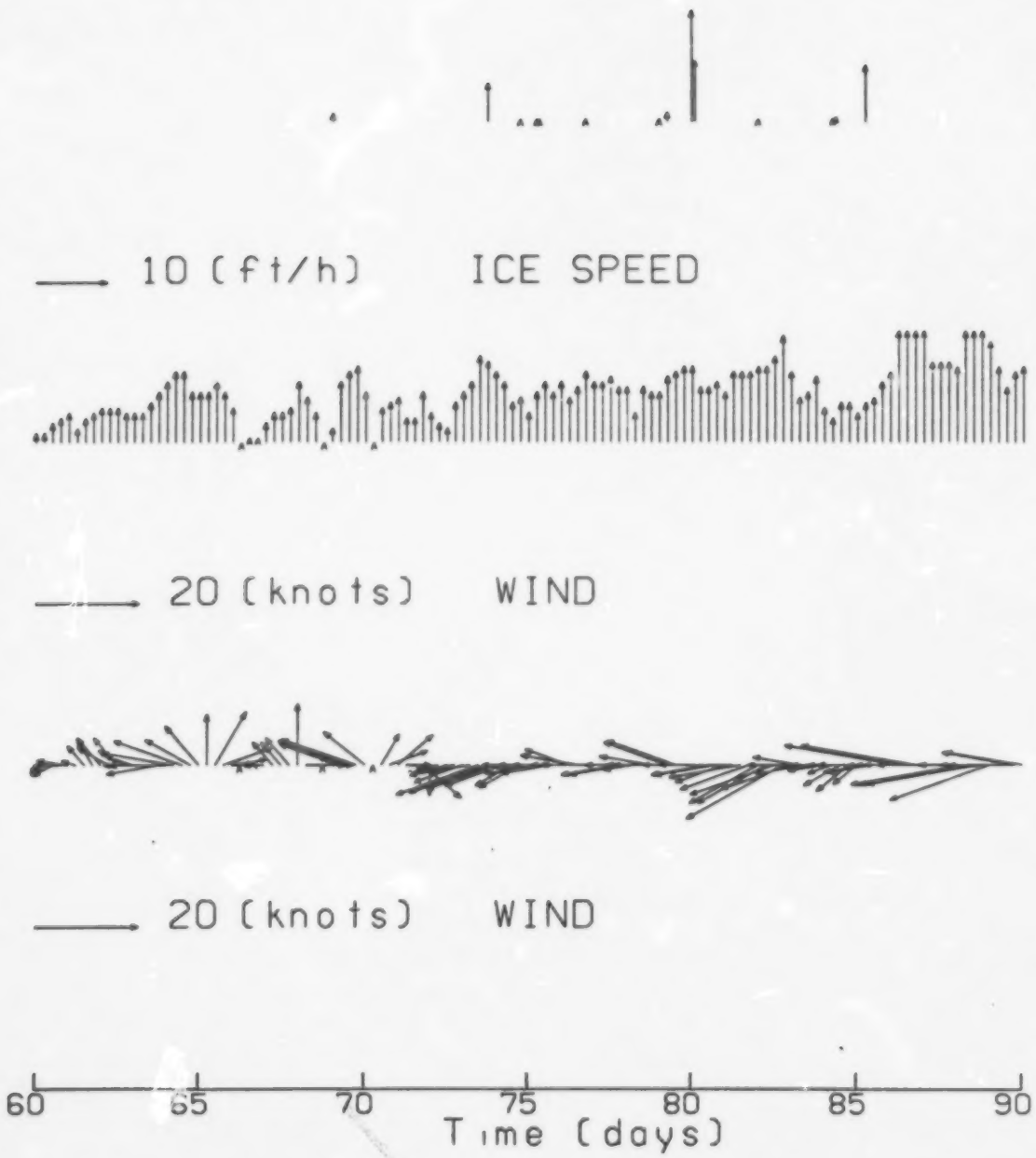


**Figure 5.3 Wind and landfast ice velocities for 1975. Dates are given in Julian days.**

- A wind speed threshold for movement events existed but there was not a direct relation between the magnitudes of the wind and ice displacements above their respective thresholds.
- The movements were primarily back and forth oscillations with a period of a few days.
- The magnitude of the movements did not decrease appreciably during the winter.
- There was a preferred axis along which motion occurred.
- A large onshore movement in early January led to an increased onshore/offshore component of movement over the the following 2.5 months.
- Wind direction did not correlate well with ice movement direction.
- Ice movements later in the winter (eg. March and April 1975) had relatively constant magnitudes.

From the above analysis, the following characteristics of the wind record were suggested as indicators of landfast ice events:

(i) wind velocity exceeding a critical threshold;
(ii) a critical change in wind speed;
(iii) a significant shift in wind direction;
(iv) the duration of wind speed over a threshold; and
(v) a preferred wind direction resulting in landfast ice motion.

Defining a movement event to result from a minimum displacement of 1.2 m, the simultaneous use of a threshold (i) and a wind direction change (iii)

was investigated. With this rule, it was possible to predict the number of events but the timing of most of the wind and movement events did not coincide. This model was therefore inadequate.

A second model applying a threshold (i) and a change (ii) was applied with more accurate predictions of numbers of events and their timing. This model was defined by:

(i) an ice event, a displacement of more than 0.5 m;
(ii) a wind peak, the highest 6 h averaged wind in a continous series equal to or above a threshold wind speed;
(iii) a wind trough, the lowest 6 h averaged wind between events; and
(iv) a wind event, when a wind peak exceeds the preceeding wind trough by a critical difference.

Calibrating with the 1974-1975 Netserk data, using a critical wind speed of 4.5 m/s and critical trough to peak difference of 4.5 m/s, this model was accurate in predicting the number of elastic displacements to within 1 percent. Significant differences were only found in the case of permanent displacements observed during the calibration period. Modelling the pack ice using the method described in section 3.5 showed that significant pack ice pressures occurred at the beginning of January 1975, coinciding with a large (1.5 m) southerly landfast ice movement.

The above model was applied to the years 1972 to 1976 during the periods for which landfast ice displacement data was available, resulting in

a prediction of 197 displacement events. Examination of landfast ice movement data shows that the frequency of events at a water depth of 4.3 m (Netserk) was within a few percent of this prediction. The measured frequency of movement events at deeper water depths increases by almost an order of magnitude but changing of the critical values in the model does not alter the predicted number of events significantly. Successful application of this model to deeper water might involve changing the threshold displacement defining an ice event and accounting for pack ice pressure.

## 5.4 Landfast Ice Speed

The above event model was not extended to include actual landfast ice velocities. Rather, this distribution was synthesized from the motions recorded by Spedding (many APOA reports here). Spedding's data covers the years between 1971 and 1978, typically covering the months from November to May in which landfast ice was present. This data is applicable in the present case since it was acquired at locations not far from the Amauligak and Kaubvik sites.

On average, hourly ice speeds of 0.15 m/h (0.5 ft/h) were detectable from the data. The frequency of these events is given in Table 5.1 and the distribution of ice speeds is given in Table 5.2 for different water depths. Kaubvik is in approximately 20 m of water while the depth at Amauligak is about 32 m. The data were not comprehensive for depths >18 m, therefore the results for >12 m were considered.

Table 5.1 Frequency of hourly landfast ice events (>0.5 ft/h) for Canadian Beaufort Sea from Spedding (1973, 1975a, 1975b, 1977)

| Water Depth | Hours of Record | Number of Events | Average per Hour | Average per 30 day month |
|---|---|---|---|---|
| 0 m - 6 m | 25910 | 380 | .015 | 11 |
| 6 m - 12 m | 8952 | 276 | .031 | 22 |
| 12 m - 18 m | 5952 | 921 | .155 | 111 |
| >12 m | 7080 | 1079 | .152 | 110 |
| >18 m | 1128 | 158 | .140 | 101 |
| all depths | 41942 | 1735 | .041 | 30 |

Table 5.2 Landfast ice speed distribution (>0.5 ft/h) for Canadian Beaufort Sea from Spedding (1973, 1975a, 1975b, 1977)

| speed (ft/h) | Water Depth/(data period) 0 m - 6 m (Nov-May) | 6 m - 12 m (Dec-May) | 12 m - 18 m (Feb-May) | >18 m (Feb-May) |
|---|---|---|---|---|
| 0.5-1.0 | 298 | 218 | 549 | 111 |
| 1.0-1.5 | 48 | 32 | 241 | 21 |
| 1.5-2.0 | 14 | 10 | 92 | 3 |
| 2.0-2.5 | 7 | 8 | 19 | 1 |
| 2.5-3.0 | 5 | 1 | 8 | 4 |
| 3.0-3.5 | 0 | 1 | 1 | 1 |
| 3.5-4.0 | 2 | 1 | 2 | 1 |
| 4.0-4.5 | 2 | 0 | 4 | 0 |
| 4.5-5.0 | 2 | 1 | 0 | 0 |
| 5.0-5.5 | 2 | 1 | 0 | 2 |
| 5.5-6.0 | - | 0 | 1 | 2 |
| 6.0-6.5 | - | 0 | 0 | 1 |
| 6.5-7.0 | - | 1 | 0 | 1 |
| 7.0-7.5 | - | - | 0 | 1 |
| 7.5-8.0 | - | - | 0 | 1 |
| 8.0-8.5 | - | - | 1 | 0 |
| 8.5-9.0 | - | - | 1 | 0 |
| 9.0-9.5 | - | - | 0 | 0 |
| 9.5-10.0 | - | - | 0 | 0 |
| 10.0-10.5 | - | - | 1 | 0 |
| 10.5-11.0 | - | - | 0 | 2 |
| 11.0-11.5 | - | - | 0 | 0 |
| 11.5-12.0 | - | - | 0 | 2 |
| 12.0-12.5 | - | - | 0 | 0 |
| 12.5-13.0 | - | - | 0 | 0 |
| 13.0-13.5 | - | - | 0 | 0 |
| 13.5-14.0 | - | - | 0 | 0 |
| 14.0-14.5 | - | - | 0 | 1 |
| 14.5-15.0 | - | - | 1 | 2 |

An exponential distribution with a mean of 1.2 ft/h was fitted to the >12 m data in Table 5.2. The distribution of annual maximum landfast ice speeds was obtained using equation (2.6). From Table 4.5, the season length is 187 days at Kaubvik for an average of 686 events per season for >12 m water depths. Both the parent and the extremal distributions are shown in Figure 5.4.

From Figure 5.1, an ice thickness of 2.2 m can be assumed for extreme load calculations. This is because the thickness distribution tended toward a spike for large numbers of events. Recalling equation (5.1), force can be obtained from a number of constants, the structure diameter and the ice velocity. Since extremal ice thickness is essentially constant, the probability distribution of load is scaled directly with that of the ice speed. The one in 100 year load is simply a constant times the one in 100 year (CDF=0.99) ice speed of 15 ft. found in Figure 5.4 (based on data).

## 5.5 Future Characterization of Landfast Ice Processes

Although landfast ice growth and motion events can be predicted from the AES data bases, its presence and extent can only be obtained directly from the original ice charts or from other sources. In the present chapter, a model for the prediction of landfast ice growth was described. This illustrated that ice thickness could be predicted from surface air temperatures with some accuracy. The model used for predicting motion events was an empirical one. While it was useful for predicting the

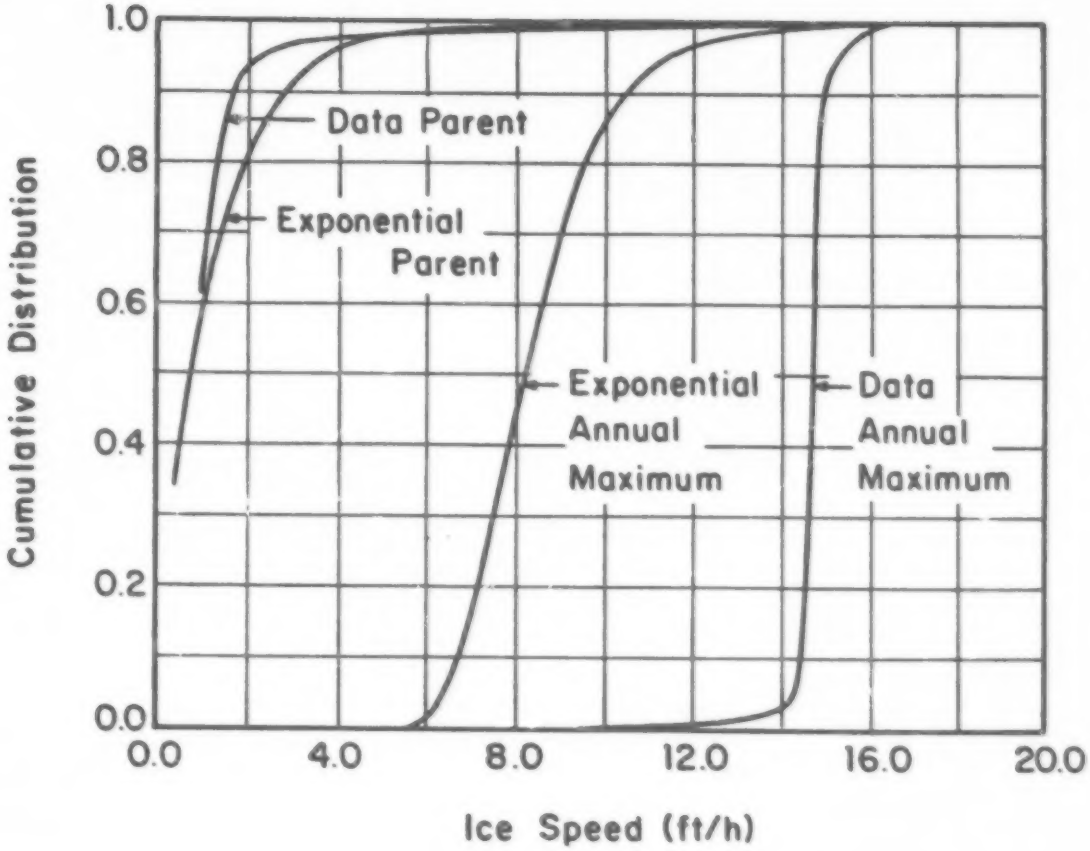


Figure 5.4 Parent and annual maximum landfast ice speed distributions at Kaubvik

occurrence of elastic deformation events, the magnitudes of motion and the corresponding velocities require site specific geometrical information on the ice cover. This information includes a detailed map of the coastline and bathymetric charts where applicable. Also important is the extent of the landfast ice since this influences the speed and direction of the motion.

The extent of landfast ice is available from the original AES ice charts. In future, it is worth digitizing this information both for the prediction of motion as noted above and for the definition of season boundaries as described previously in chapter 4.

# 6. FIRST YEAR PACK ICE

## 6.1 Ice Concentration

First year pack ice (scenario FP) can cause significant loads against structures such as the Molikpak at Amauligak (Jefferies and Wright, 1988). At offshore sites such as this, the water depth prevents the buildup of a grounded rubble field to diffuse ice loads. The pack ice is in constant motion and ice velocities reaching 0.5 m/s are possible. Late winter first year ice thickness can reach and exceed local landfast values because of advection from other areas.

Because of the tendency for ice to fracture, the forces exerted by impacting floes depend on the confining pressures exerted by the neighbouring pack ice. The occurrence of large pack ice pressures is difficult to predict. Nevertheless, significant pack ice pressures only occur when ice concentration reaches 9+/10 and 10/10 coverage. The winter distribution of all ice coverage is given for Amauligak and Kaubvik in Figure 6.1. The distribution at Kaubvik was very similar. Note that the distributions correspond to the all winter season lengths detailed in section 4.5. Since multiyear ice represents a small portion of all the ice present, the coverage of all ice and first year ice are interchangeable. It is reasonable to assume that the highest loads due to first year ice are caused by the thickest ice present. In the AES ice charts, this is given by the thick first year ice category which should be used in deriving arrival rates. Nevertheless, Jefferies and Wright (1988) found the frequency of

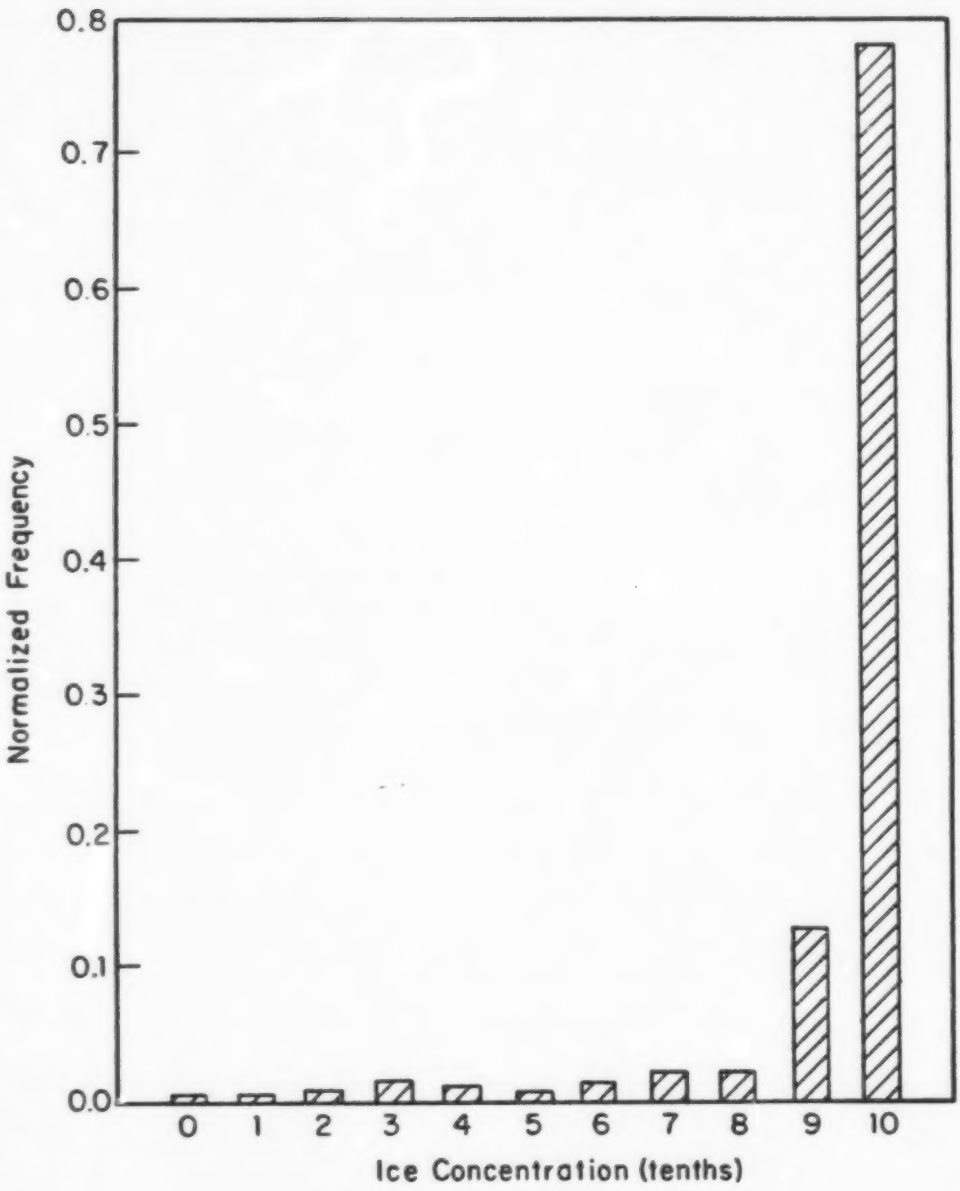


Figure 6.1 Winter distribution of total ice concentration at Amauligak for November 5 to June 30 (from SIGRID data 1972-1984)

first year ice events (>100 MN total load) to be relatively independent of date during the winter at Amauligak.

## 6.2 Ice Speed Distributions

Ice velocity is an important environmental consideration for the first year pack ice interaction scenario. High ice speeds are not required for the ice to reach its crushing strength; both crushing and flexural failure can take place at routine pack ice speeds, and peak ice pressures are less dependent on rate of loading when crushing occurs. There is, however, concern with the dynamic behaviour of structures. Continuous indentation at high speed can induce vibrations in offshore structures, increasing the potential for damage and failure.

Ice speeds can be obtained by direct measurement or derived from ice conditions and recorded winds. The first method is preferred but it involves on-ice buoy deployment or analysis of remotely sensed imagery. Many of these data for the Beaufort Sea are proprietary and efforts should be made to include this kind of information in digital data bases. An alternate approach that uses currently available AES data is presented. First year total ice concentration, c, is obtained directly from the AES Regional or the SIGRID data, depending on availability for a given date. Data for the two test sites, Amauligak and Kaubvik, were obtained through CRISP. Tuktoyaktuk winds were used for $v_a$ in the wind driven drift calculation since there is a continuous time series for much of the period between 1972 and the present. Hourly winds were used where possible. Winds

at Amauligak for selected periods between 1981 and 1984 were also used in the testing and calibration of the ice drift model. Wind time series at other offshore sites are available, but are generally of shorter duration than those at Tuktoyaktuk.

The moving pack ice is a matrix of many ice thicknesses caused by the advection of ice into the area or by the refreezing of leads. On a case by case basis, it is possible to use this information for estimating the ice resistance. For calculating velocity distributions as in the present situation, the effort would be prohibitive and quite unnecessary. As an estimate of the maximum first year ice thickness, the local landfast ice thickness was used. Ice thickness, h, was calculated using the approach described in section 3.4. This involved the accumulation of freezing degree days at Tuktoyaktuk and then applying the model developed by Parker (1987) for Kugmallit Bay.

Values used for the remaining parameters of the equations in this section are given in Table 6.1. Drift of the first year ice pack was calculated from local winds by the approach described in section 3.5. The key elements of this model are described in Figure 3.10. When ice motion is onshore, it is wind driven until the concentration reaches 10/10 and is consolidated at the structure. For offshore motion, the ice is wind driven. Many sensitivity tests were conducted to show the influence of model parameters on the final velocity distributions. There are two key elements to the model:

Table 6.1 Ice parameter values

| Parameter | Value | Units | Description |
|---|---|---|---|
| $\rho_a$ | 1.3 | kg $m^{-3}$ | air density |
| $C_a$ | 0.001 | | air drag |
| $\rho_w$ | 1030 | kg $m^{-3}$ | water density |
| $C_w$ | 0.005 | | water drag |
| $d_f$ | 200 | km | max fetch length or pack ice extent |
| $d_g$ | <50 | km | maximum width of flaw lead adjacent to landfast ice |
| q | 40000 | $Nm^{-1}$ | ice strength constant |
| $d_s$ | <5 | km | distance of site to edge of landfast ice |
| $c_m$ | 0.5 | tenths | weak fraction of ice present in 10/10 ice cover |

(i) the scaling factor g that is the ratio of calculated ice velocity to wind driven drift velocity and is a measure of the ice resistance to motion; and

(ii) the ratio of air drag to water drag coefficients used to obtain the wind driven drift.

The scaling factor was found to be insensitive to ice strength and thickness characteristics. Cases in which g was not 0 or 1 had a negligible effect on the ice speed distributions. Ice motion data from February and March 1983 was used to verify the model. On a case by case basis, g was found to be most sensitive to the ice concentration c, distance from the edge of the landfast ice $d_s$ and the direction normal of the shore. Prediction errors therefore tended to be due to geometrical assumptions. Improvements here could be made using more detailed information on the landfast ice extent. An important result to come out of this analysis was that the ice was stationary or nearly so 20 to 30 percent of the time.

The drag coefficients were the key parameters for moving pack ice. For wind speeds less than 10 m/s, ice drift is approximately 2 percent of wind speed. For higher winds, this value is closer to 4 percent (e.g. Marcellus and Morrison, 1982). Predicted ice drift speed distributions are summarized in Table 6.2. The mean values can be coupled with the fraction of time that coverage exceeds 9/10 and used to obtain an effective arrival rate. The cumulative distributions shown in Figure 6.2 are used for estimating peak speeds.

Table 6.2 Winter ice drift at Amauligak

| Site | Season | Source | Mean (m/s) | Standard Deviation (m/s) |
|---|---|---|---|---|
| Beaufort Sea | All winter | Marcellus and Morrison (1982) | .066 | .055 |
| Amauligak | All winter 05 Nov-30 Jun | Predicted Tuk winds | .058 | .050 |
| | | Predicted Amaul. winds | .075 | .071 |
| Amauligak | Early winter 05 Nov-05 Feb | Predicted Amaul. winds | .075 | .077 |
| | | Predicted Tuk winds | .054 | .051 |
| Kaubvik | All winter 02 Nov-30 Jun | Predicted Amaul. winds | .074 | .070 |
| Kaubvik | Early winter 02 Nov-25 Dec | Predicted Amaul. winds | .077 | .077 |

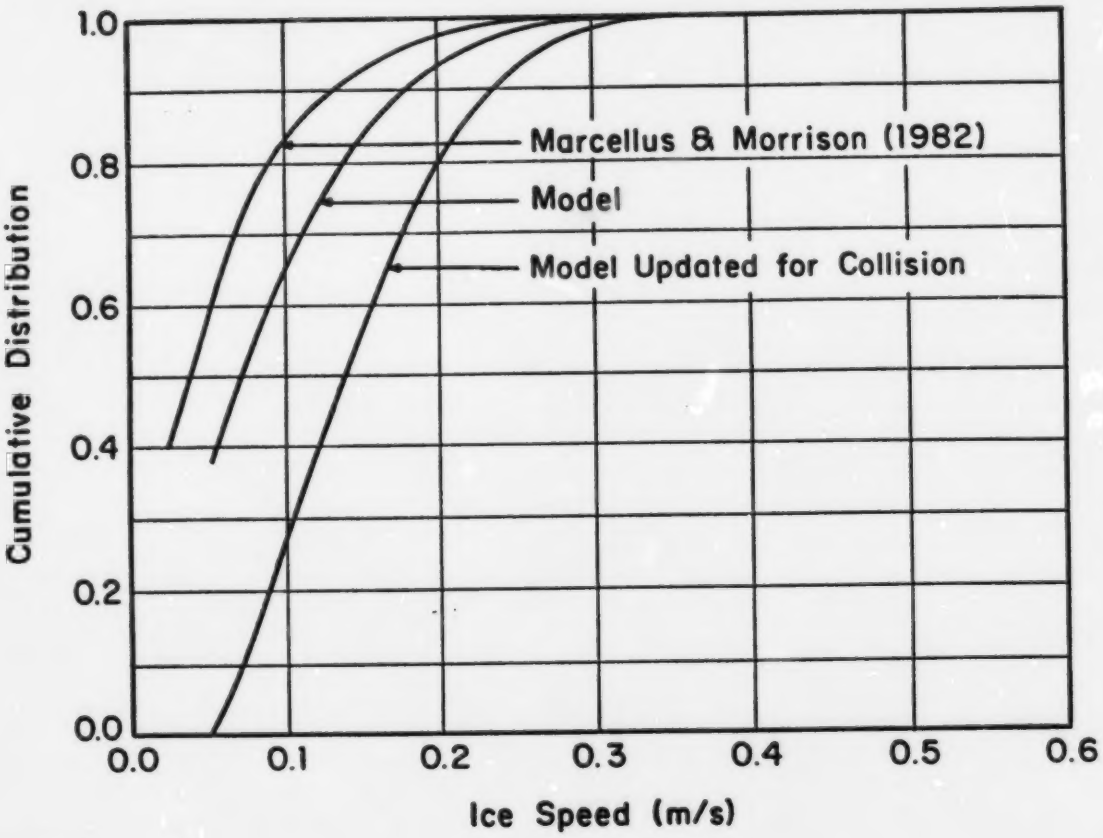


Figure 6.2 Probability distribution of winter ice speed
(a) Marcellus and Morrison from RAMS buoy data
(b) estimated using method of section 3.5
(c) estimated with update according to collision probability

## 6.3 Thickness of Moving First Year Ice

Because it is constant motion, the first year ice in the shear and transition zones (Figure 1.1) is composed of many thicknesses. This is the result of the opening of large leads in tension, ridges in compression and many smaller leads in shear. Extreme ice loads are due to the thickest level ice present and to pressure ridges.

Landfast ice grows continuously during the course of the winter. Its thickness is therefore representative of the maximum thickness of the first year pack ice. Reference should be made to section 5.2 for this distribution. Offshore at Tuktoyaktuk the distribution over 13 years of record is lumped between 1.7 m and 2.1 m, yet the maximum thickness never exceeded 2.2 m. Without loss of accuracy, a fixed value of 2.2 m can be used for the maximum thickness of the first year pack ice when many events during the year are considered. For a small number of events, the results shown in Figure 5.1 can be used.

Although ridge thickness can be related to the thickness of the parent ice sheet (e.g. Tucker and Govoni, 1981), the uncertainty in the distribution of level ice thickness during the course of the year makes this approach unrealistic. Ridge height or thickness distributions must be measured directly as in Wright and Schwab (1979) and Wright et al. (1982). Ridge frequencies can be obtained from such sources as Wright and Schwab (1979) and Spedding (1979). First year ridge heights are estimated to

average 0.9 m with a standard deviation of 0.9 m and follow an exponential distribution. If underwater slope angles are the same as above, the corresponding ridge thickness would be 3.6 to 3.9 times the sail height. Ratios larger than this have been measured, particularly for multiyear ridges in which the sails have been eroded (Dickins and Wetzel, 1981).

## 6.4 First Year Ice Load Example

An approximate 1 in 100 year ice load for moving first year ice (FP) is estimated in this section. From the wind speed records, duration statistics (DUST) were generated for winds greater than 10 m/s (20 knots). The number of these storm events per year that is pertinent to the load calculation is then

$$\nu = P(v>10 \text{ m/s})\ P(c>9+/10)\ P(\text{FP scenario})\ t_s/\bar{t} \qquad (6.1)$$

where $t_s$ is the season length and $\bar{t}$ is the mean storm duration. The derivation of (6.1) is straightforward. An event is assumed to occur each time the wind exceeds a threshold, taken here as 10 m/s. The multiplication of the probabilities requires that the three processes be independent. This is not an significant constraint and might be investigated in future. Pack ice pressure is included by only considering situations in which the ice cover is +9/10 and 10/10.

The expected number of first year pack ice events calculated from (6.1) is summarized in Table 6.3. The primary difference in the results between

Table 6.3 Wind events for first year pack ice (FP scenario) at Amauligak and Kaubvik

| Wind Source | Average duration > 10 m/s | p(v> 10 m/s) | site | p(c>9+/10) | p(FP in a given year | Expected number of events /year |
|---|---|---|---|---|---|---|
| Amauligak (1981-1985) | 7.79 | .20 | Amauligak | .77 | .85 | 73 |
| | | | Kaubvik | .78 | .25 | 21 |
| Tuktoyaktuk (1972-1986) | 4.08 | .047 | Amauligak | .77 | .85 | 33 |
| | | | Kaubvik | .78 | .25 | 10 |

the two offshore sites, Amauligak and Kaubvik, was due to the probability that the FP scenario occurred in a given year. The winds at Amauligak and Tuktoyaktuk were uncorrected for local effects and no factor was applied to the Tuktoyaktuk winds to account for differences between onshore and offshore speeds. The difference between the two wind sources was emphasized calculating p(v>10 m/s) for the Tuktoyaktuk winds, multiplied by a constraint factor of 1.35, the ratio of mean offshore to onshore winds. The probability that v>10 m/s was still only half that for Amauligak.

Many factors enter into the evaluation of ice loads. Consider as an example a situation in which the momentum parameter of the ice pack, defined as "hv", is critical; the ice load can be determined from

$$y = kvh \tag{6.2}$$

where k is a constant. The distribution of momentum can be obtained as follows. First of all, the distribution of ice thickness is weighted by the probabilities $p_1$ and $p_2$ of the level and ridged ice respectively (section 6.3)

$$f_H(h) = p_1(f_H(h))_{level} + p_2(f_H(h))_{ridged} \tag{6.3}$$

A simple solution for the distribution of momentum was obtained by applying a numerical integration technique to (6.2).

This result for the parent ice thickness distribution and the ice speed

distribution updated for collision is given in Figure 6.3. If 73 events (wind >10 m/s) occur on average per year, the distribution of annual extremes for momentum is given by the shifted curve (broken line) in Figure 6.3. The CDF=0.99 or 1/100 year value is 1.9 $m^2/s$ which can be multiplied by the constant factor k to obtain the 1 in 100 year ice load.

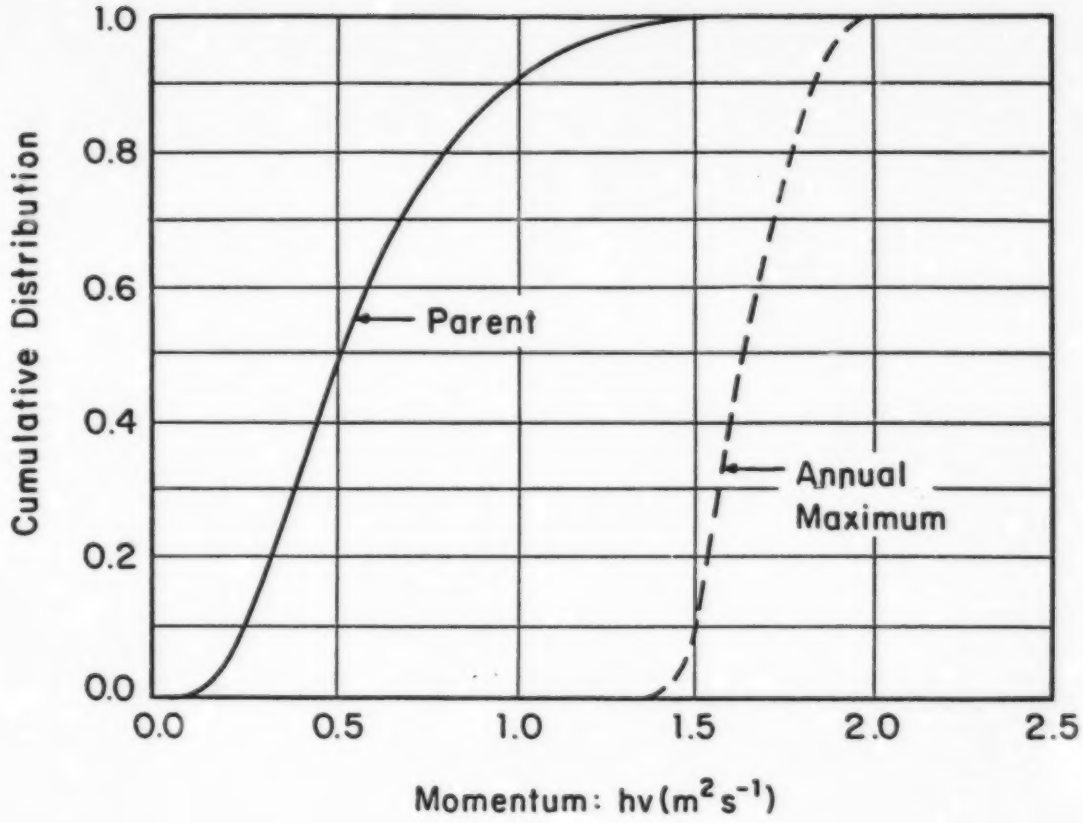


Figure 6.3 Annual extremal distribution of momentum parameter (hv) for prediction of first year pack ice loads at Amauligak

# 7. MULTIYEAR ICE

## 7.1 Multiyear Ice Events

The most serious ice load conditions in the Beaufort Sea have been caused by multiyear ice. This was evidenced by the near failure of the Molikpaq structure at Amauligak during the spring of 1986 (Jefferies and Wright, 1988). Multiyear floe impacts can occur both in summer (denoted as scenario MS) and in winter (MP). In both cases the floes can be treated as discrete arrivals, but in winter there is the additional influence of the surrounding pack ice. The important environmental parameters for the multiyear ice scenarios are:

(i) the velocity distribution used both for impact speed and arrival rate;

(ii) the arrival rate, derived from the multiyear ice concentration, floe size and velocity distributions;

(iii) the floe size distribution, used for impact energy and momentum calculations, and

(iv) the ice thickness, considering not only the thickness of the level ice, but the dimensions and frequency of ridges.

AES data bases can play an important role when determining multiyear

ice concentrations and velocity distributions. In the following sections, these are discussed along with a cursory description of floe characteristics. The approach for calculating extremal distributions of multiyear ice loads is illustrated using data for the Amauligak site.

## 7.2 Multiyear Ice Concentration

Multiyear ice concentration is a direct multiplicative factor for determining the arrival rate of multiyear floes as shown in section 2.4. Observed concentrations tend to be low and therefore subject to large natural variability and measurement error. The probability density function of the winter concentration at Amauligak is shown in Figure 7.1. The distribution is exponential but also has a peak at c=4/10. This was due to a few specific events but may also reflect a bias in the original ice charts.

Seasonal concentrations for the Amauligak and Kaubvik sites are given in Table 7.1. Summer concentrations were much lower and more variable than in the winter. The coefficients of variation (mean/standard deviation) for multiyear ice concentration were characteristically in the range of 2 to 5.

The most significant feature of Table 7.1 is the difference between the mean summer concentration for the SIGRID and AES Regional data sets. No comparison was possible for the winter season since the AES Regional data was only collected in summer. The difference is not due to the different periods of record; for the common years 1972 to 1980, the results were very

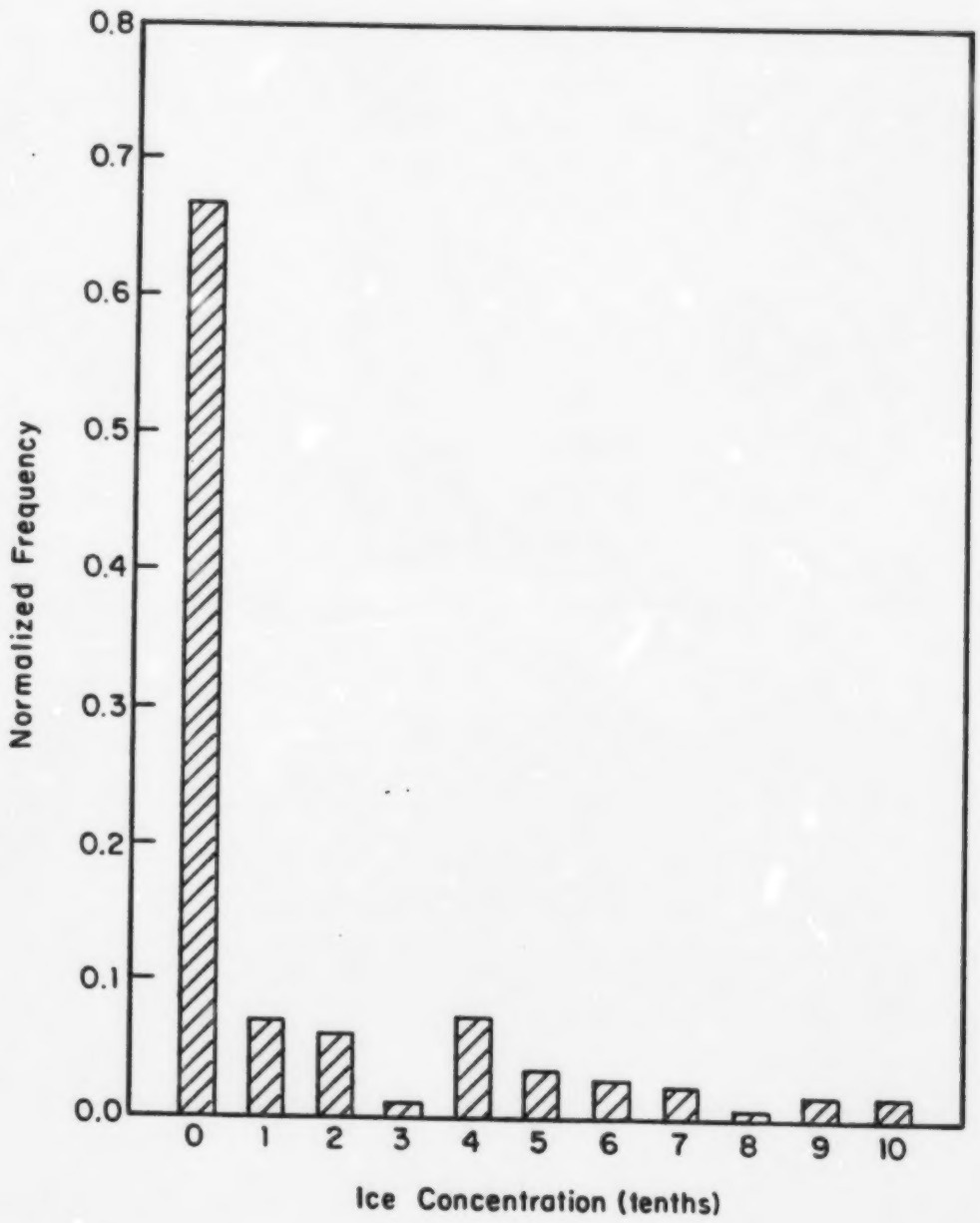


Figure 7.1 Distribution of multiyear ice concentration at Amauligak for Nov 5th to June 30th (from SIGRID data 1972-1984)

Table 7.1 Multiyear ice concentrations

| Site | Season | Source of Data | Mean (tenths) | Standard Deviation (tenths) |
|---|---|---|---|---|
| Amauligak | Summer (MS) 30 Jun-05 Nov | SIGRID | 0.21 | 0.96 |
| | Summer (MS) 30 Jun-05 Nov | AES Regional | 0.66 | 1.68 |
| | Early Winter (MP) 05 Nov-05 Feb | SIGRID | 1.52 | 2.57 |
| | All Winter (MP) 05 Nov.-30 Jun | SIGRID | 1.33 | 2.46 |
| Kaubvik | Summer (MS) 30 Jun-02 Nov | SIGRID | 0.15 | 0.72 |
| | Summer (MS) 30 Jun-02 Nov | AES Regional | 0.43 | 1.44 |
| | Early Winter (MP) 02 Nov-25 Dec | SIGRID | 1.08 | 2.17 |
| | All Winter (MP) 02 Nov.-30 Jun | SIGRID | 1.19 | 2.35 |

similar to those shown. Neither is the difference due to the spatial resolution of the data since there is more similarity between the two sites for a given data set than there is between data sets at one site. The difference appears to be directly in the source data used for the original ice charts.

These considerations emphasise the need to include in digital data bases multiyear ice concentrations from SAR radar imagery of the ice that discriminates between first year and multiyear ice. Proprietary and public data exists for the Beaufort and other Canadian arctic regions.

## 7.3 Multiyear Ice Speeds

Although the winter multiyear ice is thicker than the surrounding first year ice, its motion is very similar. Both respond quickly to changes in the wind and any inertial motions of the multiyear ice are attenuated by the first year ice matrix. The calculation of winter ice speeds is described in section 6.2, Table 6.2 and Figure 6.2.

The drift of multiyear floes in summer is unimpeded by surrounding pack ice. Ice speed is first of all required for determining arrival rate; the primary goal is to obtain the average speed at which floes move and therefore the area covered by their tracks (see section 2.4). The second requirement is for obtaining impact velocities. While arrival rate is based on the full velocity distribution, speeds of concern are related only to the maximum values.

Marcellus and Morrison (1982) have documented summer ice drift speeds around drill rigs in the Canadian Beaufort Sea; these are summarized in Figure 7.2. For winds exceeding 10 m/s (20 knots), ice motion was approximately 4 percent of wind speed and 3.5 percent on average over all wind speeds. McKenna et al. (1987) found that the factor was just over 2 percent for winds of 5 m/s. The predicted curve (b) of Figure 7.3 was based on a constant ratio of ice speed to wind speed of 2 percent at 5 m/s, increasing to 4 percent at 10 m/s.

Faster floes have a greater chance of impacting a structure. This is accounted for using a Bayesian updating scheme in which the probability densities are scaled according to the corresponding velocity. The predicted cumulative distribution updated in this manner is also shown in Figure 7.3.

## 7.4 Multiyear Floe Characteristics

Simplifying the characteristics of multiyear floes, the following features are important for design load calculations:

(i) floe size distribution;

(ii) thickness distribution of the level ice in multiyear floes, and

(iii) the ridge or hummock thickness distribution and the average fraction of floe area that these cover.

As with ice concentration, many of the above characteristics can be derived from SAR imagery. Since these are absent from the digital data bases, the following sources are used. Marcellus and Morrison (1982) report the floe

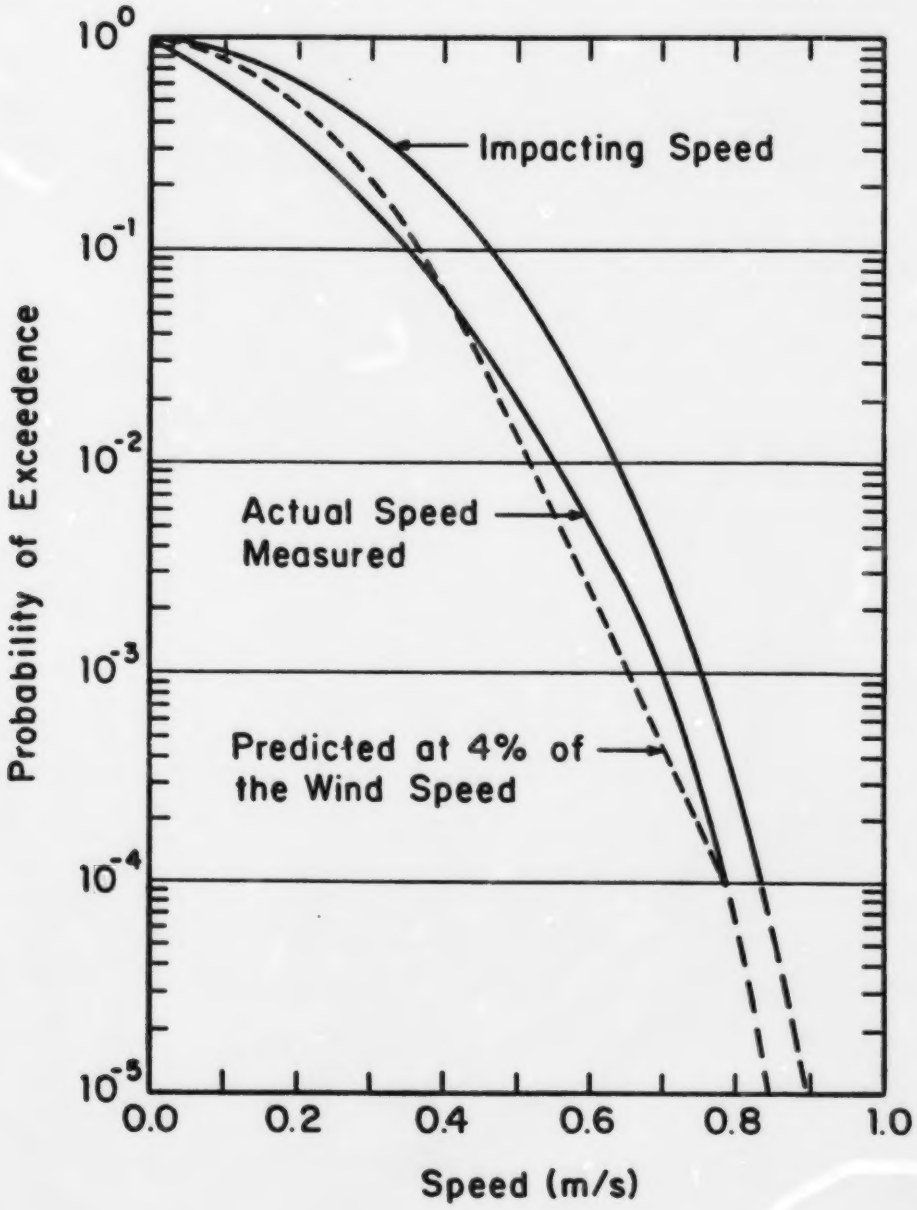


Figure 7.2 Probability of exceedance for summer ice speed (from Marcellus and Morrison, 1982)

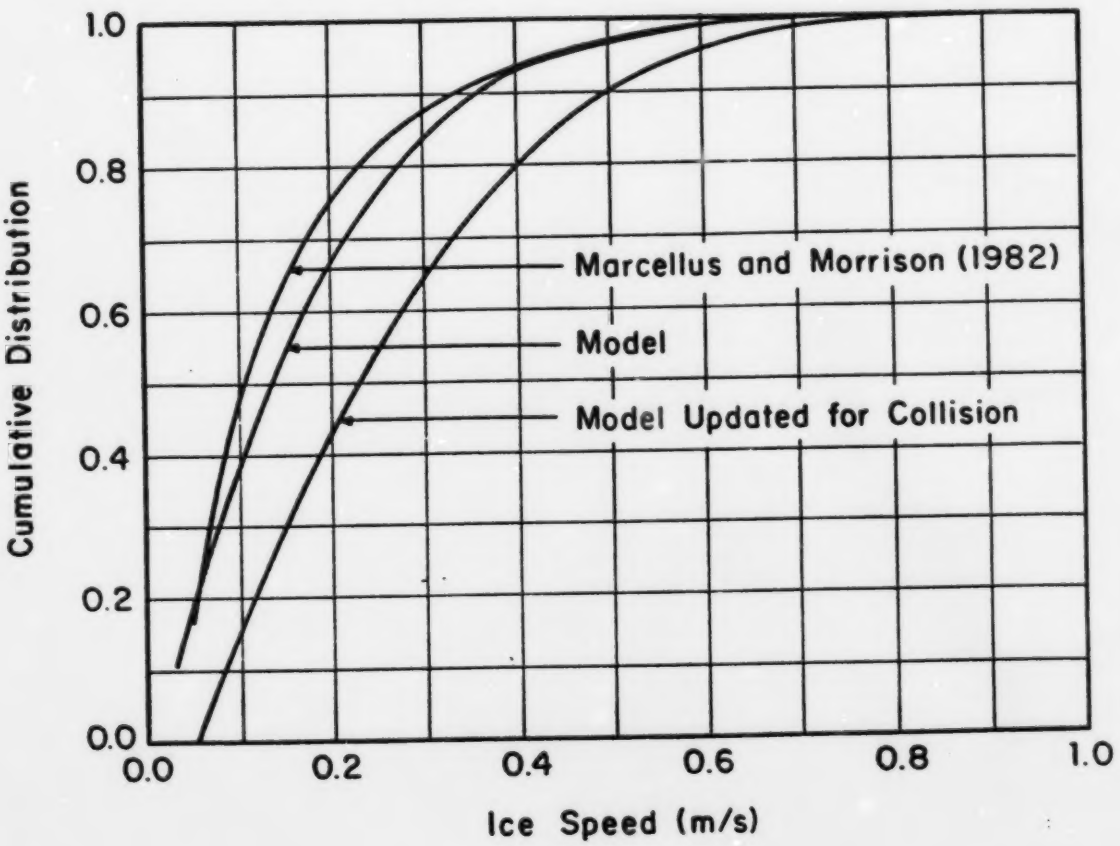


Figure 7.3 Cumulative distribution function of summer ice speed. (a) Marcellus and Morrison (1982) from observed drift at offshore rigs (b) predicted and (c) predicted with updating according to collision probability.

size distribution for floes larger than 0.5 km (Figure 7.4). Distribution of floe diameters for summer ice were also estimated by Weeks et al. (1977) near Point Barrow and Cape Simpson for floes greater than 100 m diameter. Spedding (1979) also recorded floe diameters that have been fitted to a gamma distribution with a mean of 100 m and a standard deviation of 150 m. Truncating the distribution from the Spedding data at 100 m resulted in a good fit to the Weeks et al. (1977) data.

The level ice thickness distribution was determined from submarine traces reported in Marcellus and Morrison (1982) (from De Paoli et al., 1982) and from direct measurement by AIDJEX (1976). A gamma distribution was fitted to the latter data set with a mean thickness of 3.9 m and a standard deviation of 1.6 m. This ice had a mean thickness 0.5 m less than for the submarine data.

Ridges in the multiyear ice were originally formed when the ice was young, therefore the same distribution was used as for the first year ice. The ratio of ridge thickness to sail height is greater for multiyear ice than for first year ice because of the erosion of the sails over time (Dickins and Wetzel, 1981). The fraction of floe area covered by ridged ice was estimated at 0.3.

## 7.5 Multiyear Ice Load Example

Because of the shorter landfast ice season at Amauligak than at Kaubvik, the severity of multiyear ice loads is expected to be greater. The

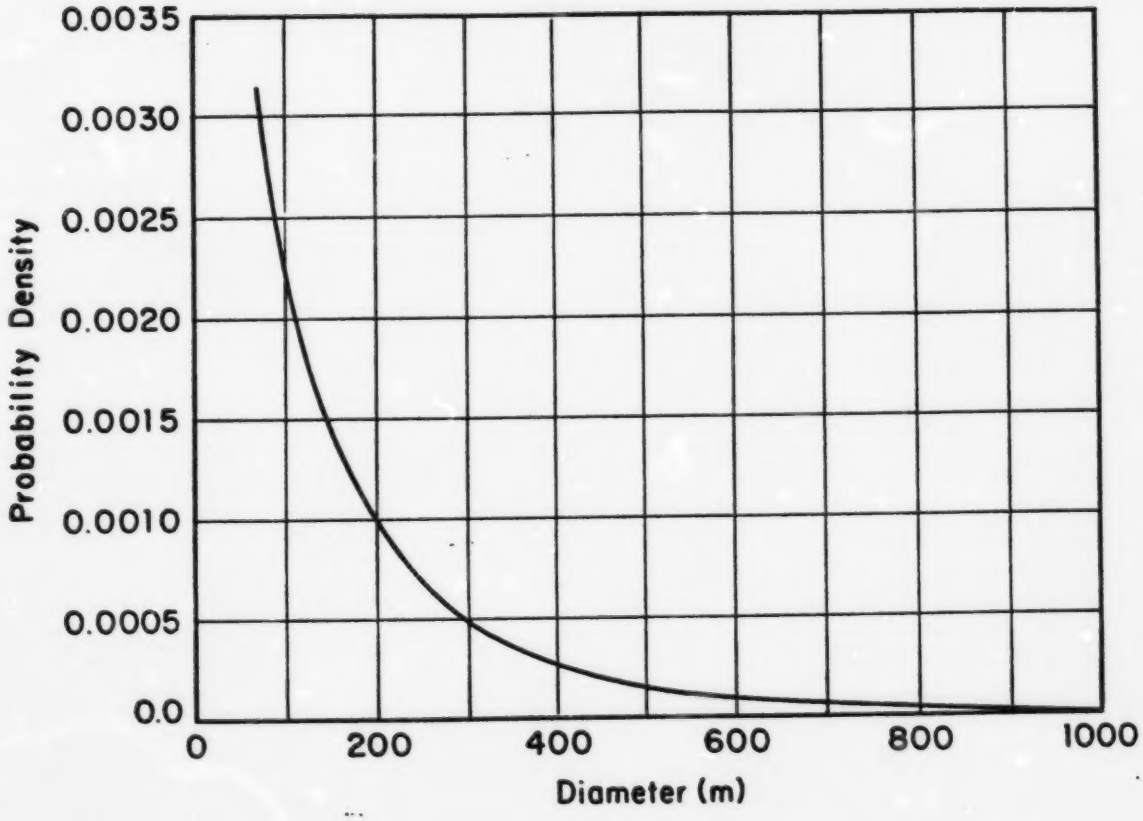


Figure 7.4 Gamma distribution fitted to the Spedding (1979) data for multiyear floe size distribution.

following load example is for Amauligak during the summer.

The force that a freely floating multiyear floe exerts on a structure can be estimated from its initial kinetic energy and the geometry of the contact. This is because most of the energy is dissipated by frictional processes as the ice crushes. Ignoring added mass and other secondary effects, the incoming kinetic energy of a floe is

$$E_K = 1/2\ \rho a h v^2 \qquad (7.1)$$

where $\rho$ is the ice density, a is the floe area, h is the ice thickness and v is the floe speed. Distributions for a and h are given in section 7.4 and for v in section 7.3. The cumulative distribution for $E_K$ was found from the convolution of the parameter distributions in (7.1) using a numerical integration approach and is shown in Figure 7.5.

The distribution of annual extremes for summer floe impact energy was calculated by modifying the parent distribution above for the expected number of floes at Amauligak. If multiyear ice concentration and speed are independent, then from section 2.4,

$$\nu = (\bar{b}+w/\bar{a})\bar{c}\ \bar{v}\ t_s \qquad (7.2)$$

where the overbars represent mean values, c is multiyear ice concentration, b is the floe diameter, w is the structure width, a is the floe area and $t_s$ is the season length.

For c=0.021 (Table 7.1), w=100 m, $\bar{b}$=100 m, $\sigma_b$=150 m (section 7.4), $\bar{a}$=0.25$\pi$($\bar{b}^2$+$\sigma^2_b$), $\bar{v}$=0.15 m/s (updated for collisions section 7.3), and $t_e$=128 days (Table 4.5), the mean number of impacts $\nu$=273/year. Applying equation (2.6), the distribution of annual maximum kinetic energy for scenario MS is given in the Figure 7.5. From this CDF, the 1 in 100 year kinetic energy is 3800 MJ.

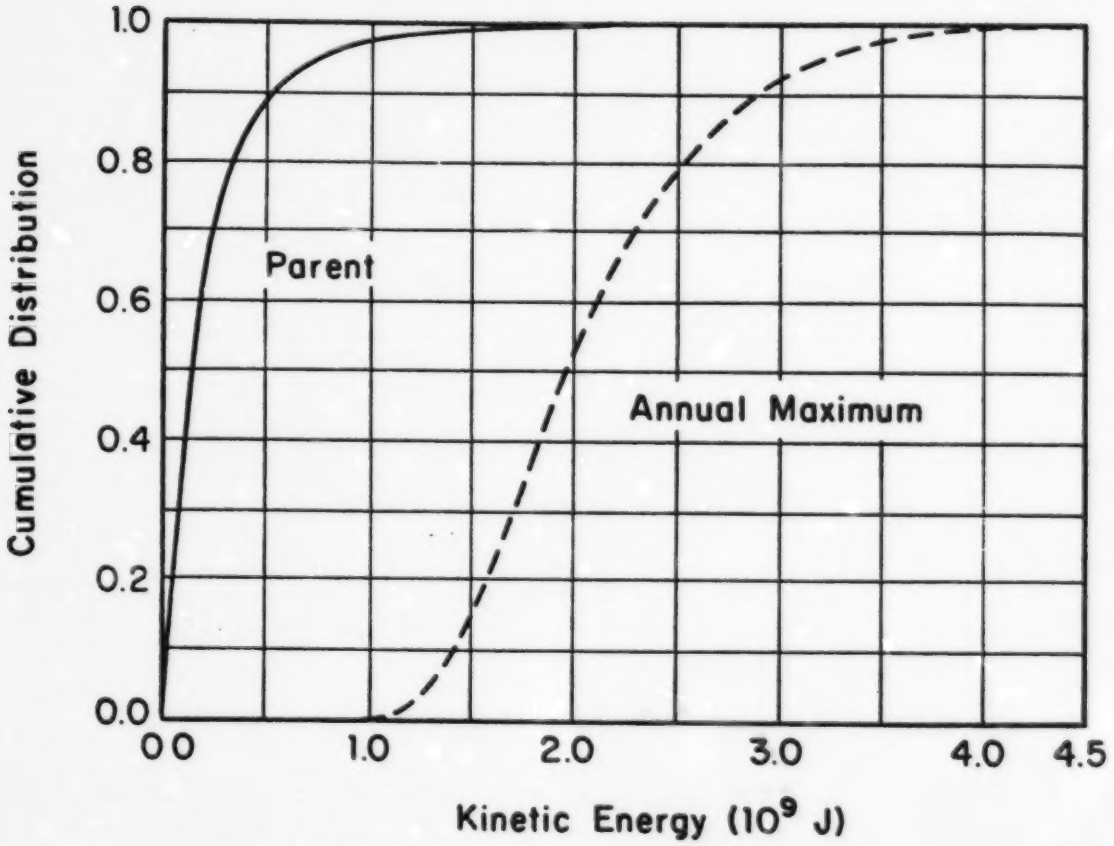


Figure 7.5 Cumulative distribution of kinetic energy for freely floating multiyear floe impacts at Amauligak during summer.

# 8. CONCLUSIONS AND RECOMMENDATIONS

## 8.1 Concluding Remarks

An approach for applying environmental parameters from AES data bases to the design of offshore structures is presented in this report. As a reference, four ice interaction scenarios are proposed:

FL first year landfast ice;

FP first year pack ice;

MS freely floating multiyear floes; and

MP multiyear floes surrounded by first year pack ice;

each with an associated period during the year in which it is likely to occur. Although each design scenario was treated in a different manner, there was a common thread in the approach used for extremal analysis. The primary goal in design is to ensure a sufficient safety level of the structure. This is accomplished by assessing the risk of failure associated with the major structural components due to many factors, including environmental loads. The distribution of the extreme loads, typically expressed as annual maxima, is therefore required. AES environmental data bases were used to define parent parameter and load distributions, and the extremal distributions were then estimated from the expected number of events occurring during a year. Events can occur annually on a rare, occasional or frequent basis. In the case of pack ice, the events tend to be either occasional or frequent. One aspect of ice speed distributions that was considered was the need to update the distributions according to collision probability. This is a basic transformation that is required for most ice

design speeds.

The load that ice can exert on offshore structures depends on both structure design and on environmental parameters. Although the latter issue is the focus of this report, it is possible to obtain extremal distributions of momentum of the pack ice and kinetic energy of discrete floes. This kind of information is one potential product of ice information systems.

For discrete features such as multiyear floes, the number of interaction events depends on their expected arrival rate. Although not exploited in the examples illustrated, the arrival rate depends on the covariance between ice concentration and floe speed. The present work can be related to a recent study on ice load determination (DnV, 1988), particularly in the area of load combinations. The chance of different load scenarios acting at the same time can be assessed from joint distributions of parameters such as wind speed, ice concentration, ice speed and air temperature.

Several key environmental parameters were obtained from the CRISP, MAST and DUST packages that assisted in the calculation of design loads. These included:

(i) ice coverage, first year and multiyear;

(ii) air temperature, used for ice growth calculation; and

(iii) wind speed distribution and duration, used for the calculation of ice velocity and storm events.

Two offshore sites in the Beaufort Sea were selected to illustrate the above

procedures. Amauligak was selected because of its offshore location and exposure to moving first year and multiyear ice. Kaubvik, although some distance offshore, is landfast during most winters. Most of the ice data for these sites were obtained from the SIGRID digital data base. Although the spatial resolution of the data is good, it was not always accurate for resolving the outer extent of the landfast ice. This was a key consideration in establishing the relative importance of the different scenarios at a given site.

Of considerable interest to engineers is the presence of multiyear ice. While it is well characterised in the data bases, differences between the concentrations from the SIGRID and AES Regional sources needs to be resolved. The thickness of both first year and multiyear ice was not measured directly, but inferred from other sources.

The specification of seasons corresponding to the ice scenarios FL, FP, MS and MP was made considering natural changes in the ice concentration and air temperatures. These were well defined using information accessed from the CRISP and MAST packages.

As implied in the recommendations that follow, landfast ice extent and motion are not well covered in the SIGRID and AES Regional data bases. An attempt was made to relate landfast motion events to winds but this requires further study.

Where the AES data bases did not provide complete information, several

physical and empirical models were presented to transform and enhance the data into forms usable for design calculations. These included:

(i) criteria for the definition of season boundaries;

(ii) an ice growth model from air temperature;

(iii) a wind induced ice drift model; and

(iv) a landfast ice displacement event model.

While offshore structure design requires site specific information, arctic shipping requires a more varied geographical distribution that is also provided by the CRISP package. Examples of arctic shipping models are ASPEN (Ferregut et al, 1988; Daley et al, 1987) and the DnV model (Jordaan et al, 1987; Jordaan 1987). ASPEN presently uses monthly and seasonal data on a 15 nautical mile grid for first year ice thickness and concentration, old ice thickness and concentration, floe size, ridge height and frequency, iceberg numbers and iceberg sizes.

## 8.2 Recommendations

Several steps are considered to improve the environmental input for load calculations. First of all, many sources of data are still confidential and it will take some time before these are available in the public domain. These data include local ice speeds and records of ice loading events. A significant amount of SAR aircraft radar imagery flown by Intera Technologies Ltd. of Calgary for various offshore operators is available for the Beaufort Sea. Other SAR imagery flown for the Canadian Coast Guard and Canarctic Shipping is also available (Canadian Arctic Marine

Atlas, 1987). From these data, excellent multiyear floe size distributions, ice concentrations, ice ridge distributions, landfast ice extent and ice speeds can be obtained.

More specific to the extremal techniques outlined in this report, the CRISP package can be enhanced to provide direct input to environmental load calculations. Some suggestions to achieve this are:

(i) the calculation of joint probability distributions between parameters - examples of this might be multiyear ice concentration given greater than 9/10 all ice coverage or ice speed and multiyear ice concentration;

(ii) the ability to generate distributions of extremal values of ice speed when available; and

(iii) the fitting of standard probability distributions to such parameters as ice thickness, floe size and ice concentration- this is particularly important since the distributions are best generated directly from the digital data and are key inputs for load calculations.

Ice loads are but one part of the offshore design scenario and must be considered in combination with other factors such as winds, waves and earthquakes. Load combination procedures have been outlined for fixed offshore structures in CSA (1988). The verification of these and the development of standards for other situations in the offshore necessitates the calculation of joint distributions between ice loading parameters and loading parameters for other processes. Many of the same ice load

parameters are also relevant to arctic shipping problems. Although less emphasis is placed on ice speeds, geographical variability is more important and visibility criteria are accentuated. CRISP can potentially be expanded to consider these problems.

Some particular physical features of the ice pack were addressed in the report and may require further investigation:

(1) When dealing with offshore sites near the boundary between the landfast ice and the moving pack ice, the spatial resolution of the data is critical. Even distances of 10 km can make significant differences in the ice regimes present. Currently, landfast ice is not specified in the digital data; its addition would be a useful contribution for design considerations. Floe sizes, particularly for the multiyear ice, can have a significant effect on the loads exerted on offshore structures. Future efforts in the digitization of ice charts should bear this in mind. If attempts have been made to ground truth ice thicknesses with the stage of development recorded on the ice charts, this information would be of considerable use for load calculations and for the inference of ice motion.

(2) Events in which large pieces of landfast ice break off can be a significant hazard to structures. These events were only given a cursory mention in this report; their frequency and magnitude are worth future consideration.

(3) Ridges are the thickest features in the first year and multiyear pack ice, and therefore represent some of the greatest dangers to

structures. Information on their magnitude and frequency of occurrence is worth including in digital data bases.

(4) For the case where multiyear ice is moving in first year pack ice (scenario MP), conditions are more severe for shipping and for structures if the ice field is converging. Wind and ice cover data could be used to determine the probability of converging, diverging or stable ice conditions. This is an interesting area for new research.

(5) The relation between parameters at different locations (i.e. their spatial relation) can be used to enhance otherwise insufficient information. A good example of this that has already received some attention is the relation between winds at various sites. Many ice and meteorological parameters can be characterised in this way.

(6) The measurement of every parameter of concern for design calculations is not always possible. We must therefore rely on physical and empirical relations between parameters for this information. The calibration of models such as those describing landfast ice events and pack ice drift proposed in this report are potential candidates for further study.

## 9. REFERENCES

Agerton, D.J. and Kreider, J.R. 1979. "Correlation Of Storms And Major Ice Movements In The Nearshore Alaskan Beaufort Sea" POAC, Trondheim, Norway.

Agnew, T., Maxwell, B. and Mathews, T. 1987. "An Ice and Snow Climate Information System", Third International Conference on Interactive Information and Processing Systems for Meteorology, Preprint Volume, American Meteorological Society.

AIDJEX. 1976. "Ice Thickness", AIDJEX Bulletin No. 32, pp.65-68.

Baird, W.F. and Associates, Hydrotek and Lawless, J.F. 1986. "Review and Assessment of Procedures for Extreme Value Analysis for Selected Geophysical Data", Canadian Climate Centre Report 86-12, Atmospheric Environment Service, Downsview, Ontario.

Canadian Arctic Marine Atlas. 1987. Transport Canada Report No. TP-8318-E, prepared by Canarctic Shipping Co. Ltd. for Canadian Coast Guard Northern, 66p.

Canadian Standards Association. 1988. "General Requirements, Design Criteria, Environment and Loads: Part I - CSA Code for the Design, Construction and Installation of Fixed Offshore Production Structures", CSA-S471, Eighth Draft.

Colony, R. and Thorndike, A.S. 1984. "An Estimate of the Mean Field of Arctic Sea Ice Motion", Journal of Geophysical Research, 89(C6), 10623-10629.

Coon, M.D. 1980. "A Review of AIDJEX Modelling, Proceedings of ICSI/AIDJEX Symposium on Sea Ice Processes and Models", University of Washington, 12-27.

Daley, C., Perchanok, M., Ferregut, C. and Brown, R. 1987. "ASPEN Model Update to 1987", Transport Canada Report TP-8554-E prepared by Arctec Canada Ltd. for Canadian Coast Guard Northern, 93p.

de Finetti, B. 1974. "Theory of Probability", Vols. 1 and 2 (translated from Italian by Machi, A. and Smith, A.), Wiley, New York.

de Paoli, S., Morrison, T.B. and Marcellus, R.W. 1982. "Analysis pf Interaction Probabilities Between Large Ice Features and Offshore Structures in the Canadian Beaufort Sea", Beaufort EIS.

Det norske Veritas. 1988. "Probabilistic Framework for Ice Loads on Fixed Marine Structures", Det norske Veritas report submitted to Department of Public Works Canada, DSS Contract No. EN280-7-0733/01.

Dickins, D.F. and Wetzel, V.F. 1981. "Multi-Year Pressure Ridge Study Queen Elizabeth Islands", Proc POAC 81, Quebec.

Dunwoody, A.B. 1983. "The Design Ice Island for Impact Against an Offshore Structure", Proceedings of Offshore Technology Conf., OTC 4550, Vol. 2, pp. 324-330.

Ferregut, C., Perchanok, M., and Daley, C. 1988. "Ship/Ice Probabilities in Arctic Shipping", in proc. Ninth Int. Conf. on Port and Ocean Engineering under Arctic Condtions (POAC 87), Fairbanks, Alaska, Vol. 1. pp.631-643.

Hibler, W.D., III. 1979. "A Dynamic Thermodynamic Sea Ice Model", Journal of Physical Oceanography, 9(4), 815-846.

Jefferies, M.G. and Wright, W.H. 1987. "Dynamic Response of 'Molikpak' to Ice-Structure Interaction". Int. Conf. on OMAE, 1988.

Jordaan, I.J. 1983. "Risk Analysis With Application to Fixed Structures in Ice", Seminar/Workshop on Sea Ice Management, Memorial University of Newfoundland, St. John's, Newfoundland.

Jordaan, I.J. 1986. "Statistical and Probabilistic Aspects", Keynote address to Workshop on Ice-structure Interaction, Calgary, Alberta, May/June. Sponsored by Public Works Canada and Centre for Frontier Engineering Research, Edmonton, Alberta.

Jordaan, I.J. 1987. "Probabilistic Analysis of Environmental Data for Design of Fixed and Mobile Arctic Offshore Structures", Reliability and Risk Analysis in Civil Engineering, Proceedings of ICASP5, the Fifth International Conference on Applications of Statistics and Probability in Soil and Structural Engineering, Vancouver, B.C., May 25-29, Vol. 2, pp. 1130-1137.

Jordaan, I.J. and Maes, M.A. 1984. "Probability, Exchangeability and Extremes: with a discussion of Iceberg Loading". Civil Engineering Systems, Vol. 1, pp.234-241.

Jordaan, I.J., Nessim, M.A., Ghoneim, G.A. and Murray, A.M. 1987. "A Rational Approach to the Development of Probabilistic Design Criteria for Arctic Shipping", in proc. Sixth International Offshore Mechanics and Engineering Symposium (OMAE 1987), Houston, Vol. IV, pp.401-406.

Marcellus, R.W. and Morrison, T.B. 1982. "Ice Design Statistics for the Canadian Beaufort Sea", C.M.E.L. Report No. 1015 prepared for The EIS Partners.

Markham, W.H. 1983. "Artificial Islands and Fast Ice", Department of Environment (Canada) Report on Coastal Ice Conditions in the Beaufort Sea.

McKenna, R.F. 1986. "Spatial Analysis of Pack Ice Motion", Ph.D. Thesis, University of Waterloo, 189p.

McKenna, R.F., Thomson, N.R. and Sykes, J.F. 1987. "Uncertainty of Summer Ice Drift Forecasts", in proc. Ninth Int. Conf. on Port and Ocean Engineering Under Arctic Conditions (POAC 1987), Fairbanks, Alaska.

McKenna, R.F., Sykes, J.F. and Lennox, W.C. 1983. The Influence of Changes in Constitutive Law on Sea Ice Motion, Proc. Seventh Int. Conf. on Port and Ocean Engineering Under Arctic Conditions, Helsinki, Finland, pp.172-179.

McPhee, M.G. 1986. "Analysis and Prediction of Short-Term Ice Drift". Proc. OMAE '86, Tokyo, Japan, 385-393.

Murray, A. and Maes, M.A. 1986. "Beaufort Sea Extreme Wave Studies Assessment", Environmental Studies Revolving Funds, Report No. 023, 97p.

Overland, J.E. 1985. "Atmospheric Boundary Layer Structure and Drag Coefficients Over Sea Ice". J. Geophys. Res., 90(C5), pp.9029-9049.

Parker, M.N. 1987. "Ice Thickness Climatology for Northern Canada", Report 87-1, Scientific Services, A.E.S. Western Region.

Ponter, A.R.S., Palmer, A.C., Goodman, D.J., Ashby, M.F., Evans, A.G. and Hutchinson, J.W. 1983. "The Force Exerted by a Moving Ice Sheet on an Offshore Structure", Cold Regions Science and Technology, Vol. 5, pp.109-118.

Richardson, F.A. and Burns, B.M. 1975. "Ice Thickness Climatology for Canadian Stations". Atmospheric Environment Service.

Sea Ice Climate Information System. 1986. "CRISP User's Manual", Canadian Climate Centre, Atmospheric Environment Service, 241p.

Snyder, D.L. 1975. "Random Point Processes", Wiley and Sons.

Spedding, L.G. and Croasdale, K.R., 1972. "Landfast Ice Movement - Mackenzie Delta 1972" APOA Project 33, Imperial Oil Ltd., 1972

Spedding, L.G. 1973. "Landfast Ice Movement-Mackenzie Delta 1972-73", APOA Project 51, Imperial Oil Ltd.

Spedding, L.G. 1974. "The Extent and Growth Pattern of Landfast Ice in the Southern Beaufort Sea - Winter 1972-73", APOA Project 54, Imperial Oil Ltd.

Spedding, L.G. 1975. "Landfast Ice Movement - Mackenzie Delta 1973-74", APOA Project 67, Imperial Oil Ltd.

Spedding, L.G. 1975. "Landfast Ice Movement Mackenzie Delta 1974/75", APOA project 83, Imperial Oil Limited.

Spedding, L.G. 1977. "Landfast Ice Movement Mackenzie Delta 1975/76", APOA Project 105, Imperial Oil Ltd.

Spedding, L.G. 1979. "Landfast Ice Motion Observed In The Mackenzie Delta Region Of The Southern Beaufort Sea In The 1972/73 Winter", POAC, Trondheim, Norway.

Spedding, L.G. 1981. "Landfast Ice Motion Observed in the MacKenzie Delta Region of the Southern Beaufort Sea in the 1972/73 Winter". Coastal Engineering, 5:193-209.

Spedding, L.G. 1982. "Landfast and Shear Zone Ice Conditions in the Southern Beaufort Sea - Winter 1977/78", Beaufort E.I.S. Support Document.

Spedding, L.G. 1983. "A Large Landfast Ice Movement". In Proceedings POAC '83, Helsinki, Vol. 3, pp.203-213.

Spedding, L.G. and Hawkins, J.R. 1985. "A Comparison of the Effects of Natural Meteorological Conditions and Artificial Islands on Regional Ice Conditions in the Beaufort Sea", Proc. POAC '85, Narssarssuaq, Greenland, Vol. 1, pp.305-315.

Thomson, N.R., Sykes, J.F. and McKenna, R.F. 1987. "An Application of Short Term Ice Modelling to the Beaufort Sea", accepted for publication in Journal of Geophysical Research.

Thorndike, A.S. and Colony, R. 1982. "Sea Ice Motion in Response to Geostrophic Winds", Journal of Geophysical Research, 87(C8), 5845-5852, 1982.

Tucker, W.B., Weeks, W.F., Kovacs, A. and Gow, A.J. 1980. "Nearshore Ice Motion At Prudhoe Bay, Alaska", Arctic Ice Dynamics Joint Experiment, Univ. of Washington Press, Seattle.

Tucker, W.B., III and Govoni, J.W. 1981. "Morphological Investigations of First-Year Sea Ice Pressure Ridge Sails", Cold Regions Science and Technology, Vol. 5, pp.1-12.

Walden, J.T., Hallam, S.D., Baldwin, J.T. and Thomas, G.A.N., (1987); "Prediction of Multiyear Ice Impact Loads Utilising Hans Island Data", Proc. 9th. International Conference on Port and Ocean Engineering under Arctic Conditions, Fairbanks, Alaska.

Weeks, W.F., Kovacs, A., Mock, S.J., Tucker, W.B., Hibler, W.D. & Gow, A.J. 1977. "Studies Of The Movement Of Coastal Sea Ice Near Prudhoe Bay, Alaska, U.S.A.", Journal of Glaciology, Vol 19, No. 81.

Weeks, W.F., Tucker, W.B. III, Frank, M. and Fungcharoen, S. 1977. "Characterization of Surface Roughness and Floe Geometry of Sea Ice Cover the Continental Shelves of the Beaufort and Chukchi Seas".

Wright, B.D., Gupta, P. and Lussenburg, Y. 1982. "Beaufort Sea Ice Stereo Photo Analysis: 1979-1981", Gulf Canada Resources Inc.

Wright, B.D. and Schwab, D.L. 1979. "Beaufort Sea Ice Stereo Photo Analysis: 1973-76", Gulf Canada Resources Inc.

Wright, B.D. and Schwab, D.L. 1979. "Beaufort Sea Ice Stereo Photo Analysis: 1977-78", Gulf Canada Resources Inc.